A climate-change attribution retrospective of some impactful weather extremes of 2021

Davide Faranda[1,2,3], Stella Bourdin[1], Mireia Ginesta[1], Meriem Krouma[1], Robin Noyelle[1], Flavio Pons[1], Pascal Yiou[1], and Gabriele Messori[4,5]

[1]Laboratoire des Sciences du Climat et de l'Environnement, UMR 8212 CEA-CNRS-UVSQ, Université Paris-Saclay, IPSL, 91191 Gif-sur-Yvette, France
[2]London Mathematical Laboratory, 8 Margravine Gardens London, W6 8RH, UK
[3]LMD/IPSL, Ecole Normale Superieure, PSL research University, Paris, France
[4]Department of Earth Sciences and Centre of Natural Hazards and Disaster Science (CNDS), Uppsala University, Uppsala, Sweden
[5]Department of Meteorology and Bolin Centre for Climate Research, Stockholm University, Stockholm, Sweden

Correspondence: Davide Faranda (davide.faranda@cea.fr)

Abstract. The IPCC ~~report~~ AR6 ~~indicates~~ report outlines a general consensus that anthropogenic climate change is modifying the frequency and intensity of ~~class of~~ extreme events such as cold spells, heatwaves, storms or floods. A ~~different point of view is to investigate whether~~ pertinent question is then whether climate change may have affected the characteristics of a specific extreme event~~would have~~ , or whether such event would have even been possible in the absence of climate change~~, or whether climate change may have affected its specific characteristics~~. Here, we address this question by performing an attribution of some major extreme events that occurred in 2021 over Europe and North America: the winter storm Filomena, the French Spring cold spell, the Westphalia Floods, the Mediterranean summer heatwave, ~~the~~ hurricane Ida, the Po Valley tornadoes outbreak, ~~the~~ medicane Apollo and the late autumn Scandinavian ~~cold-spell~~cold spell. We focus on the role of the atmospheric circulation associated with the events and its ~~likelihood~~ typicality in present (factual world) and past climate conditions (counterfactual world) ~~—~~ defined using the ERA5 dataset 1950 to present. We ~~use an analogs-based methodology whose aim is to find~~ first identify the most similar sea-level pressure patterns to the ~~target events~~ extreme events of interest in the factual and counterfactual worlds ~~and~~ — so-called analogues. We then compute significant shifts in ~~probability~~the spatial characteristics, persistence, predictability~~and seasonality of the patterns~~, seasonality and other characteristics of these analogues. We also diagnose whether in the present climate the ~~analogs~~ analogues of the studied events lead to warmer/cooler or dryer/wetter conditions than in the past. Finally we verify whether the El-Nino–Southern Oscillation and the Atlantic Multidecadal Oscillation may explain interdecadal changes in the analogues' characteristics. We find that most of the ~~events~~ extreme events we investigate are significantly modified in the present climate with respect to the past, because of changes in ~~position~~the location, persistence and/or seasonality of cyclonic/anticyclonic patterns ~~. Two~~ in the sea-level pressure analogues. One of the events, ~~storm Filomena and~~ Medicane Apollo, appears to be a black swan of the atmospheric circulation, with ~~analogs of bad quality~~poor-quality analogues. Our approach, complementary to the statistical ~~methods already available in the community, warns that the~~ extreme event attribution methods in the literature, points to the potentially important role of the atmospheric circulation ~~should be taken into account when performing~~ in attribution studies.

Copyright statement. TEXT

1 Introduction

One of the main novelties of the latest IPCC AR6 report (Allan et al., 2021) with respect to previous IPCC documents is the increased confidence that anthropogenic climate change is critically affecting ~~the dynamics of weather extremes. For summer, the~~ weather extremes. As stated by the IPCC AR6~~report states~~ , "a warmer climate will intensify very wet and very dry weather and climate events and seasons, with implications for flooding or drought (high confidence), but the location and frequency of these events depend on projected changes in regional atmospheric circulation, including monsoons and mid-latitude storm tracks". Similarly, the already very clear statements of the previous reports on changes in temperature extremes are confirmed and strengthened: "In all continental regions[...] and at the continental scale, it is very likely that the intensity and frequency of hot extremes will increase and the intensity and frequency of cold extremes will decrease". Other studies underline that we are already observing prolonged periods of extremely warm conditions (Horton et al., 2016) with increased droughts leading to forest fires (Flannigan et al., 2000), species extinctions (Román-Palacios and Wiens, 2020) and health issues for vulnerable populations (Mitchell et al., 2016). ~~In~~ Recent scientific literature points to the need of understanding the role of dynamical drivers of changes in weather extremes: in winter, increased persistence of cyclonic and anticyclonic structures ~~leads~~ can lead to extremely wet ~~and~~ or dry periods ~~(Ogawa et al., 2018), the latter associated with foggy weather and smog accumulation in urban areas (Sachweh and Koepke, 1995; Hu et al., 2020). Finally, the IPCC also warns~~ (Berkovic and Raveh-Rubin, 2022) on the Eastern Mediterranean. Such change in persistence of synoptic structure is also expected to change with global warming in the northern hemisphere summer(see, e.g. Kornhuber and Tamarin-Brodsky (2021)). Gordon et al. (2005); Bala et al. (2010) and Pendergrass et al. (2017) suggest that, in the shoulder seasons, we observe a large variability of rains associated with both tropical and extratropical storms and convective events, leading to an alteration of the hydrological cycle ~~(Gordon et al., 2005; Bala et al., 2010; Pendergrass et al., 2017). These trends are expected to accelerate in the coming years, if the global efforts to reduce carbon emissions are not implemented swiftly (Trisos et al., 2020)~~ .

While these assessments are meaningful when considering (relatively) large ensembles of extreme events with similar characteristics, it is also important to evaluate whether the probability of occurrence, or physical characteristics, of ~~a single extreme event~~ single extreme events have been influenced by anthropogenic climate change. This knowledge builds awareness of the consequences of greenhouse gas emissions in the general public, and allows stakeholders to evaluate specific impacts induced by climate change. For these reasons, attributing a single extreme event to climate change has given rise to a wealth of studies, an entire field named attribution ~~(Shepherd, 2016; Jézéquel et al., 2018; Naveau et al., 2020; van Oldenborgh et al., 2021)~~ (Shepherd, 2016; Knutson et al., 2017; Jézéquel et al., 2018; Naveau et al., 2020; van Oldenborgh et al., 2021).

Studies in extreme events attribution are conventionally grounded in extreme value theory (Trenberth et al., 2015), which they use to estimate return times of threshold exceedances of ~~particulars~~ particular observables (e.g. temperatures above or below a target value for a certain number of consecutive days for heatwaves ~~and~~ or cold-spells). The main drawback of such statistical at-

tribution is that it does not take into account the physical processes leading to the extreme events. Climate change is likely associated with complex dynamical changes in the atmosphere ~~(e.g. Stendel et al., 2021)~~(e.g. Kennedy et al., 2016; Sharmila and Walsh, 2018; , yet the conventional extreme value approach overlooks these entirely. This brought Shepherd (2014) to argue that the atmospheric circulation is a key element of the uncertainty in attribution studies, and in parallel stimulated attempts to incorporate knowledge of the atmospheric circulation into an attribution framework (Shepherd, 2016; Yiou et al., 2017).

Here, we build upon this line of work by performing an attribution of some notable extremes occurring during the 2021 calendar year, based on large-scale atmospheric drivers. In particular, we analyze: i) the winter storm Filomena which caused, in January, heavy ~~snowfalls~~ snowfall and extremely cold conditions in Spain; ii) the late winter cold spell that occurred in April 2021 in France with large impacts on vegetation and agriculture; iii) the July floods in Westphalia, Germany, responsible for the destruction of entire villages, infrastructure and heavy loss of lives; iv) the record-breaking temperatures during the August Mediterranean heatwave and the associated wildfires in Greece and Italy; v) the September Po Valley tornado outbreak; vi) Hurricane Ida, which caused ~~heavy~~ extensive damage in Louisiana and New York city; vii) ~~the~~ medicane (Mediterranean Hurricane) Apollo which ~~occurred~~ caused heavy flooding in Sicily in October; and viii) the November Scandinavian cold spell, which led to record-low temperatures for the season.

In order to attribute these events to climate change, we study the ~~concurrent~~ associated atmospheric circulation patterns and we search for pattern recurrences — which we term analogues — in the far (1950–1979) and recent past (1992–2021). Our working hypothesis is that the far past acts as a counterfactual world where the Earth's climate was less heavily influenced by anthropogenic forcing when compared to the recent past (the factual world). ~~Additionally~~Here, we assume that 30 years is a long enough period to average out ~~the~~ high-frequency interannual variability of the atmospheric motions~~(~~. However, it is necessary to control for the effect of lower-frequency and inter-decadal variability, such as that caused, for example, by the Atlantic Multi-Decadal Oscillation or by low-frequency modulations of the El Nino–Southern Oscillation~~) and the climate within these periods can be assumed (quasi)stationary with respect~~ . If a direct influence of such low-frequency variability can be excluded, then changes in analogues between the two periods we consider can be attributed to the climate change signal. We present in Section 2 the methodological aspects of this work, introducing in Section 3 the relevant assessment metrics. The Section 4 contains, for each event: (i) a ~~description,~~ meteorological description of the event, (ii) a ~~state-of-the art of climate-change aspects related to the event and~~ summary of the known impacts of climate change on that event class, and (iii) our attribution analyses. Our conclusions are presented in Section 5.

2 A method for ~~attribution of~~ attributing extreme events to climate change which takes into account changes in atmospheric circulation

We study changes in weather patterns associated with extreme events by leveraging the framework of weather ~~analogs~~analogues (Yiou et al., 2003). We first identify the peak day of each extreme event. We then perform a ~~semi-objective~~ semi-objective detection of the concurrent large-scale weather pattern using daily average sea-level pressure (slp) from the ERA5 reanalysis ~~databas cover~~ database over 1950–2021 ~~. The~~ (Hersbach et al., 2020). The choice of using slp is motivated by: i) the fact that in the

ERA5 reanalysis, this quantity is computed from real station observations and not derived from the model, ii) its capability to track and identify extratropical cyclones (Walker et al., 2020), iii) the absence of long-term trends in its values bt also on the dynamical systems metrics Faranda et al. (2019a). The semi-objectivity lies in the exact choice of geographical domain over which the pattern is identified. For cyclones, the domain of the analysis can be easily identified as the low-pressure area associated with the storm. For cold spells and heatwaves, we follow Stefanon et al. (2012), who have shown that these events have a ~~large scale~~ large-scale dynamical footprint spanning the size of the European continent. For all cases, we have tested that our method is qualitatively insensitive to modest changes in the domain size. ~~Four our analysis, we~~ We split the ERA5 dataset into two periods: 1950–1979 and 1992–2021. We take the first period to represent a counterfactual world with a weaker anthropogenic influence on climate than ~~in~~ the second period, which represents our factual world affected by anthropogenic climate change. To take into account the possible influence of low-frequency modes of natural variability in explaining differences between the two periods, we also consider the possible roles of the El-Nino – Southern Oscillation (ENSO) and the Atlantic Multidecadal Oscillation (AMO).

For each period, we scan scan all the daily average slp geographical maps and select the best 33 ~~analogs~~analogues, namely the maps minimizing the euclidean distance with respect to the map of the event itself. The number of 33 corresponds approximately to the smallest 3‰ of euclidean distances in each subset of our data. We have tested extracting between 25 and 50 analogue maps, without finding any qualitatively large differences in our results. ~~Note that for~~ For the factual period, as ~~common practise~~ is common practice in attribution studies, the event itself is removed. Furthermore, we forbid the ~~analogs~~ analogues search in a window of a week centered around the date of the event. We ~~do not restrict the analogs search to a specific season , which~~ restrict the analogues search to the extended season during which each event occurs (DJFM, MAMJ, JJAS or SOND) or to the seasons relevant for the occurrence of specific extreme events such as hurricanes or tornadoes. This allows us to identify possible seasonality shifts between the counterfactual and factual periods, yet prevents conflating the different physical processes which may contribute to a given class of extremes during the warm versus cold seasons. We then compute the average slp map for all ~~analogs~~ analogues in each of the two periods, and take the difference between the two averages (Δslp). To determine significant changes between the analogue maps of the two periods, we adopt a bootstrap procedure which consists of pooling the dates from the two periods together, randomly extracting 33 dates from this pool 1000 times, creating the corresponding difference maps and marking as significant only grid point changes ~~above~~ more than two standard deviations above or below the mean of the bootstrap sample. We also plot the 2-meter temperature ($t2m$) and daily precipitation rate fields (tp) on the dates of the closest slp ~~analogs~~analogues, repeating the same bootstrap procedure to identify significant changes. We additionally plot the distributions of several evaluation metrics in the two periods (see Sect. 3). We finally consider the seasonality of the analogues within the relevant season and their association with ENSO and AMO. We conduct the latter analysis using monthly indices computed from the NOAA/ERSSTv5 data and retrieved from KNMI's climate explorer. In particular, the ENSO index is the 3.4 version as defined by Huang et al. (2017) and the AMO index is computed as described in Trenberth and Shea (2006). When the ENSO 3.4 index is positive, it corresponds to El Nino and when negative to La Nina. To assess the significance of changes in factual vs. counterfactual distributions, we conduct in all cases a two-sided Cramér-von Mises test at the 0.05 significance level. If the p-value is smaller than 0.05, the null hypothesis

($H = 0$) that the two samples come from the same distribution can be rejected (Anderson, 1962). All relevant figure panels display the p-value ($pval$) and the result of the test H in the title.

3 Evaluation Metrics

Following Faranda et al. (2020), we define some quantities that support our interpretation of the ~~analogs-based~~ analogues-based attribution. All of these may then be compared between the counterfactual and factual periods.

- Analogue Quality Q: Q is the average euclidean distance of a given day from its closest 33 ~~analogs~~analogues (Faranda et al., 2020). One can then compare Q for the peak day of the extreme event to Q for each analogue of the extreme event. If the value of Q for the extreme event belongs to the same distribution as, or is smaller than, the values of Q for the ~~analogs~~analogues, then the extreme event has good ~~analogs~~ analogues and attribution can be performed. If instead the Q for the extreme event is larger than that of the analogue days, then this indicates a highly unusual slp configuration and the results of the attribution analysis must be interpreted with care. Differences between the counterfactual and factual periods in the value of Q for the peak day of the extreme event indicate whether the the atmosphere is visiting states (~~analogs~~analogues) that are more or less similar to the map associated with the extreme~~(i. e. how large~~ . Differences in the distribution of Q for the ~~peak day of the extreme event is), and~~ 33 analogues indicate whether those states are in turn becoming more or less "typical" of the atmospheric variability~~(i. e. whether the distribution of~~ . In order to test the homogeneity of the analogues in the two periods, we have computed Q for ~~the 33 analogs shifts towards higher or lower values).~~ all days in the factual and counterfactual periods on the wide North Atlantic domain [80W-50E and 22.5N-70N] and applied the two-sided Cramér-von Mises test at the 0.05 significance level. The pvalue found (0.1995) imply that the null hypothesis that the two samples come from the same distribution cannot be rejected, hence supporting our claim of homogeneity.

- ~~Seasonality of analogs: We can count the number of analogs in each month to detect whether there has been a shift of the circulation towards earlier or later months of the year. This can have strong thermodynamic implications, for example if a a circulation leading to large positive springtime temperature anomalies becomes more common in summer, when average temperatures are much higher.~~

- Predictability Index D: Using dynamical systems theory (Freitas et al., 2011, 2016; Lucarini et al., 2016b), we can compute the local dimension D of each daily slp map (Faranda et al. (2017b, 2019b), see Appendix A). The local dimension is a proxy for the number of degrees of freedom of the field, meaning that the higher D, the more unpredictable the temporal evolution of the slp maps will be ~~(Faranda et al., 2017a; Messori et al., 2017)~~(Faranda et al., 2017a; Messori et al., 2017; Hochman e . If the dimension D of the ~~chosen day~~ peak day of the extreme event is higher or lower than that of its ~~analogs~~analogues, then the ~~day will be~~ extreme will be respectively less or more predictable than the closest dynamical situations identified in the data. We compute two values of D for the event, one using the ~~counterfactual analogs~~ data in the counterfactual period and one using the ~~factual ones~~data in the factual period. As for Q, we also compute the ~~distribution~~ distributions

of D for all the ~~analogs~~analogues in each period. This informs on how predictable the extreme event is with respect to its ~~analogs.~~ analogues.

- Persistence Index Θ: Another quantity derived from the dynamical systems theory is the persistence Θ of a given configuration (Faranda et al. (2017b), see Appendix A). The persistence ~~counts~~ estimates for how many days we are likely to observe a map that is an analogue of the one considered (Moloney et al., 2019). As ~~explained~~ for Q and D, we compute the two values of the persistence for the extreme event in the factual and counterfactual worlds and the corresponding distributions of persistence for the ~~analogs~~analogues.

- Seasonality of analogues: We can count the number of analogues in each month to detect whether there has been a shift of the circulation towards earlier or later months of the season. This can have strong thermodynamic implications, for example if a circulation leading to large positive temperature anomalies in early spring becomes more common later in the season, when average temperatures are much higher.

- Association with ENSO and AMO: To account for the effect of natural interdecadal variability, we analyze the distributions of the ENSO and AMO indices corresponding to analogues of each event in the factual and counterfactual periods. If the null hypothesis that the two distributions do not differ between the two periods is rejected, it is not possible to exclude that thermodynamic or dynamic differences in the analogues are partly due to these modes of natural variability, rather than anthropogenic forcing. On the other hand, if it is not possible to reject the null hypothesis of equal distributions, observed changes in analogues can be attributed to human activity. It is worth noting that such null hypothesis of no influence of natural variability is coherent with the view of Trenberth (2011), who argued that *"Past attribution studies of climate change have assumed a null hypothesis of no role of human activities [...] I argue that because global warming is 'unequivocal' and 'very likely' caused by human activities, the reverse should now be the case. The task, then, could be to prove there is no anthropogenic component to a particular observed change in climate"*.

4 Results

Our list of 2021 extreme events is not intended to be exhaustive. We ~~mostly~~ cover Europe and North America, and we try to select events that differ in impacts, season and genesis in order to provide a rich overview of ~~attribution capabilities and~~ the attribution capabilities of our approach but also of its implementation difficulties. We provide in Table 1 the list of the events studied, with the ~~date for the analogs search, countries of interest and~~ peak day of each extreme used for the analogues search, affected countries, longitude-latitude ~~box for the analogs search~~ boxes used for the analogues search and months used for the analogues search. A graphical representation of the events is provided in Figure 1.

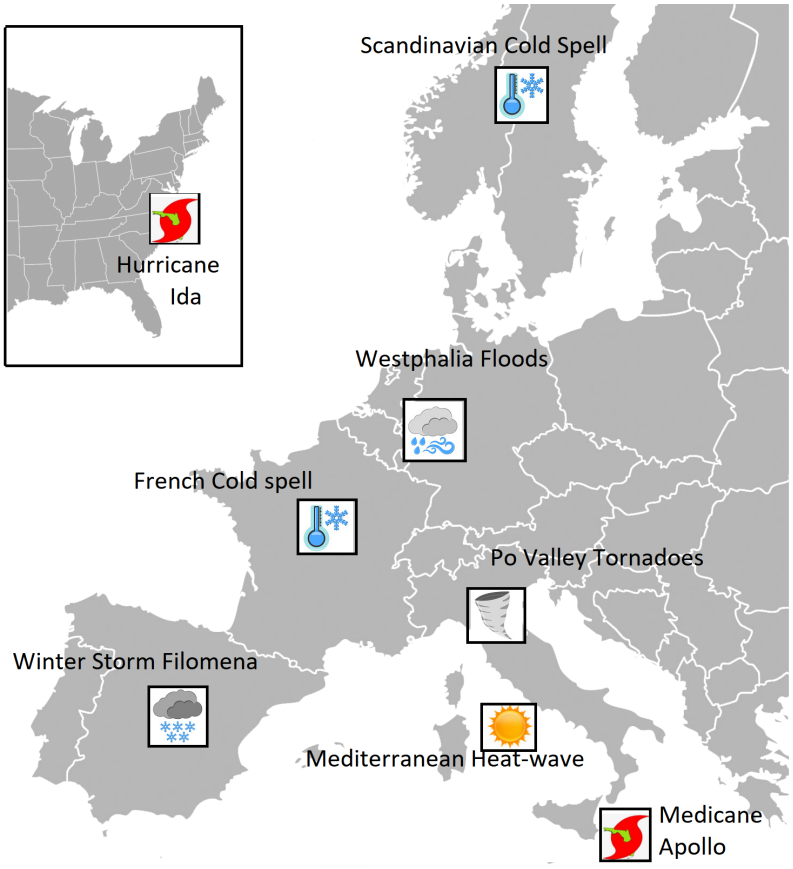

Figure 1. ~~Visual~~ Graphical representation of the events studied in this work.

Event	Date	Countries	~~analogs~~ analogues Box	analogues months
Winter Storm Filomena	09-01-2021	Spain	[15°W,10°E,30°N,46°N]	DJFM
French Spring Cold Spell	06-04-2021	France	[10°W,30°E,30°N,70°N]	MAMJ
Westphalia floods	14-07-2021	Benelux/Germany	[5°W,23°E,41°N,59°N]	JJAS
Mediterranean Heatwave	11-08-2021	Spain/France/Italy	[10°W,25°E,30°N,45°N]	JJAS
Hurricane Ida	02-09-2021	USA	[80°W,55°W,35°N,55°N]	ASON
Po Valley Tornadoes Outbreak	19-09-2021	Italy	[10°W,20°E,35°N,50°N]	MJJASO
Medicane Apollo	29-10-2021	Italy	[10°E,20°E,34°N,40°N]	SOND
Scandinavian Cold Spell	28-11-2021	Sweden/Norway	[10°W,30°E,35°N,75°N]	SOND

Table 1. List of the events presented in this study, with the ~~date~~ peak day of each extreme used for the ~~analogs~~ analogues search, affected countries~~of interest and~~ , longitude-latitude ~~box~~ boxes used for the ~~analogs~~ analogues search and months used for the analogues search.

4.1 Winter Storm Filomena

In early January 2021 the weather regime over the Euro-Atlantic sector was characterized by a negative phase of the North Atlantic Oscillation (NAO~~, see, e.g. Michelangeli et al. (1995)~~), with cold air from the Arctic being advected over southern Europe and frontal activity favoured over the Azores. Filomena was ~~named after~~ associated with an extratropical cyclone that moved from the Azores to the Canary Islands and the Iberian Peninsula on the 6th and 7th of January respectively, resulting in strong precipitation and hurricane-force winds. It triggered historic snowfalls in the inland regions of the peninsula and a 14-days long cold spell. This exceptional event caused four casualties between the 9th and the 16th of January and economic losses of up to 2 billion euros (Aon, 2021). The ~~storm~~ cyclone formed on January 1st in the northeastern inland of the United States. On January 3rd it entered the North Atlantic and it began a sharp displacement southeastward forced by a high-pressure system in the central North Atlantic and pushed by a ~~strong meridional polar jet~~ polar jet with a strong meridional component. When it reached the Azores on the 5th ~~, despite being weakened~~ in somewhat weakened form, it was ~~finally~~ named Filomena by the Spanish Meteorological Agency AEMET, which emitted a severe weather warning for Canary Islands and Spain for the two following days. The 6th and 7th of January, Filomena strengthened as it moved southeast towards the Canary Islands. The cyclone then traveled northeastward towards the Iberian Peninsula on January 7th, bringing relatively warm, humid air for the Winter season. At this time, southern Europe was experiencing cold temperature anomalies because of an anticyclone located west of the UK, resulting in temperature minimums below 0°C in almost the entire Iberian Peninsula. Hence, when the storm arrived in the Gulf of Cadiz on January 8th, its warm front blew over the preexisting cold air, allowing precipitation in the form of snow or sleet throughout most of the Iberian Peninsula, except for some parts of southern Spain. The precipitation lasted for three days, until Filomena dissipated in the Mediterranean sea on January 11th. The most affected regions were central and northeastern Spain, which accumulated an average of 30 to 50 cm of snow (AEMET, 2021b). The accumulated snow favored the persistence of low temperatures in the following days, triggering a cold spell that lasted for about two weeks, from January 5th to 17th, with a temperature average of 2°C in the Iberian peninsula and an anomaly of -3.8° with respect to the ~~1981-2010~~ 1981–2010 climatology, as recorded by the AEMET (2021b).

4.1.1 Extratropical winter storms and climate change

~~Numerous studies have addressed the influence of climate change on extratropical cyclones (ECT) due to their impacts on many regions of the planet (e.g. Zappa et al., 2013; Ulbrich et al., 2009).~~ The IPCC report ~~gathers and summarizes some of them (Lee et al., 2021) and it highlights that , by the end of the 21st century, the~~ highlights that "the number of extratropical cyclones ~~will slightly decrease, especially in~~ (ETCs) composing the storm tracks is projected to weakly decline in future projections, but by no more than a few percent change" and that "the reduction is mostly located on the equatorward flank of the storm tracks" (Lee et al., 2021). However, it also states that: "substantial uncertainty and thus low confidence remain in projecting regional changes in Northern Hemisphere jet streams and storm tracks, especially for the ~~southern flank of storm tracks. In the Southern Hemisphere, storm tracks are likely to shift poleward, while there is low confidence in the response in the Northern Hemisphere . CMIP6 models show a tripolar pattern in the~~ North Atlantic ~~storm track in winter, represented~~

by an increase in storm activity over central Europe and a decrease in Scandinavia, Southern Europe, and the Mediterranean region (Lee et al., 2021). There basin in winter". Nonetheless, "despite small changes in the dynamical intensity of ETCs, there is high confidence that the average precipitation rate of precipitation associated with ETCs will increase in a future climate in response to the increase in the atmospheric water vapor content. Snowfall associated with ECTs will decrease because of tropospheric temperature increases (Seneviratne et al., 2021). According to Seneviratne et al. (2021), the number of ECT associated with strong winds over the North Atlantic and Europe will decreasefuture" (Seneviratne et al., 2021). In addition, there is "high confidence that snowfall associated with winter ETCs will decrease in the future, because increases in tropospheric temperatures lead to a lower proportion of precipitation falling as snow" (Seneviratne et al., 2021). Besides the IPPC report, numerous studies have addressed the influence of climate change on extratropical cyclones (ETCs) due to their impacts on many regions of the planet (e.g. Zappa et al., 2013; Ulbrich et al., 2009; Priestley and Catto, 2022). Hence, there is a priori mixed evidence for the anthropogenic contribution to dynamical changes in Filomena-like storms would be less probable in a future climate and would be less likely to produce such amounts of snowfall and strong winds, although they would be associated with more precipitationstorms.

4.1.2 Attribution of Filomena to climate change

We now use the ERA5 data to perform the attribution of the cyclonic circulation associated with Filomena for the 09-01-2021 in the past and present climate climates (Figure 2). We find a significant decrease increase of the slp depression up to 3hPa for the factual with respect to the factual period (in the factual period (Fig. 2a-d). Temperatures (Figure 2e-g) are significantly and considerably warmer (h) in the recent period , specially over land, probably due to a temporal shift of the recurrence of this storm towards warmer months and an increase in surface temperatures shows that Filomena was an unusually cold event compared to its analogues even in the counterfactual period. In the factual period analogue temperatures over Iberia are significantly warmer than in the counterfactual period (Fig. 2h), by up to 4°C. This can likely be related to the long-term surface temperature warming signal in recent years. This warming does not imply a general increase in the precipitation, hence we deduce that the precipitation changes are more dynamically induced. Precipitation (l) Precipitation for the factual analogues compared to the counterfactual ones is significantly larger over southeastern Cantabrian Sea and Cape Nao, and lower in the Pyrenees, Catalonia and south in the center and center-east of the Iberian Peninsula. However, no significant differences are found in the peninsular center, peninsula, where Filomena had the highest impact. The analogs its highest impact, and in the southeast of the peninsula (Fig. 2l). On the other hand, precipitation is significantly lower in the Gulf of Lion and southwestern Mediterranean Sea.

The analogues quality Q (m) shows that this circulation pattern is highly uncommon in both periods because the quality of the event lies at the edge of the violin plots.This suggests that Filomena is somehow a black swan (Taleb, 2005), an event that has not occurred before as its analogs are distributed in a different way. The for Filomena is in the upper tail of the distribution, indicating moderate quality, and is poorer in the factual period (Fig. 2m) . There is little change in the event's predictability index D (n) increases slightly in the factual world while the Fig. 2n) with respect to the atmospheric circulation in the two periods. Still, the analogue distributions in the two periods are statistically different, with the factual period showing a shift

towards higher D values. On the contrary, the persistence Θ ~~(o) decreases, which means that storms like Filomena are more predictable and less persistent in the current climate. We see an overall decrease in frequency in Spring and an increase in Summer months.~~

~~Hence, this event would have been colder and more likely in the counterfactual world, leading to even lower temperatures and higher precipitation on the Pyrenees.We underline that the fact that analogs quality Q is poor for the event and that there are no analogs in the counterfactual nor factual world in January~~ of the event with respect to the circulation decreases (Fig. 2o), ~~make Filomena a black swan of the atmospheric circulation, an unprecedented event, emphasizing the exceptional nature of the event and the limitation of this and other attribution studies~~while no significant change is found in the Θ of the analogues. Figure 2p shows only modest changes in seasonality, with a slight increase in January and February analogues. Although Filomena occured during a negative ENSO phase, there is a significant change in the ENSO distribution for the analogues, with the factual period showing more positive values (Fig. 2q). This means that the results may be modulated by ENSO. The distributions of the AMO phases do not evidence any significant influence of this mode on the analogues (Fig. 2r).

Filomena-like storms in the factual period display higher slp yet cause more precipitation in central Spain, the region that suffered the highest impacts from the storm. Even though there are slightly more analogues in the coldest months, that is, January and February, there is a significant increase in the 2m temperature, making the snow at low altitudes less probable in a warmer climate. Given the reasonable quality of analogues, we can state that the results are in line with the expected climate change trends discussed in the previous section. However, since there is a shift in the distributions of ENSO conditioned to the analogues, we can not reject the hypothesis that ENSO variability has some influence on the analogues of Filomena.

4.2 French Spring Cold Spell

A frost event took place from 6th to 8th April 2021 in France. It was exceptional, with daily minimum temperatures below -5°C recorded in several ~~places~~locations. Grapevines and fruit trees were damaged especially in the Loire and Rhône Valleys, as frost management strategies (e.g. ~~as local~~ heating from braseros) could not be implemented in time. The temperatures broke record lows at many French weather stations. This cold event happened one week after an episode of ~~record-breaking~~ high temperatures in March ~~also in many places~~ which was also record-breaking at many locations in France (LaChaineMeteo, 2021) and Western Europe. This sequence (or compound event, according to the definition proposed by Zscheischler et al. (2020)) led the growing season to start early, with bud burst occurring in March and the new leaves and flowers left exposed to the deep frost episode that followed in early April. ~~This~~ The April cold spell was associated with an advection of cold air from the Arctic into France ~~between April 5th and 7th 2021. A~~ on April 5-6th 2021, facilitated by a deep low pressure based over Scandinavia and anticyclonic conditions overs Iceland~~, pumped cold Arctic air into France on April 5-6th 2021, which~~ . This created the low-temperature anomaly in the subsequent days.

4.2.1 ~~French cold~~ Cold spells and climate change

The IPCC AR6 describes as "virtually certain" that there have been warmer and/or rarer cold spells over most land areas since the 1950s, that this trend is due to anthropogenic climate change and that it is set to continue in the future ~~Allan et al. (2021).~~

~~Indeed, there is a large consensus the frequency and average duration of such events will eventually decrease (Russo and Sterl, 2011)~~ (Allan et al., 2021). As stated in Chapter 11 of the IPCC AR6 (Seneviratne et al., 2021, p. 1548), "a decrease in the number of cold spell days has been observed over nearly all land surface areas (Easterling et al., 2016) and in the northern mid-latitudes in particular (Van Oldenborgh et al., 2019)".

While a rapid warming, in general, lowers the probability of cold spell occurrence, projected changes in the temperature distribution imply that regional changes in cold spell frequency and/or intensity may not match changes in the mean temperature (Tamarin-Brodsky et al., 2019). Similarly, Kodra et al. (2011) have shown that long-lasting periods where temperatures drop below an absolute threshold (e.g. frost days) may still be produced locally and occasionally even in future, warmer climates. There has also been a a lively debate in the literature on whether dynamical changes associated with climate change may act to partly counter the thermodynamic changes and favour cold spell occurrence. Faranda (2019) and D'errico et al. (2019) argued that circulation patterns associated with cold spells over Europe have been increasing in frequency in the present climate and will continue to do so under future climate change. Several authors have also argued for or against a link between Arctic Amplification and an increased occurrence of cold spells in some mid-latitude regions (Mori et al., 2014; Cohen et al., 2018; Blackport and Screen, 2020; Ye and Messori, 2020; Jolly et al., 2021).

Cold spells continue to have large detrimental socio-economic effects, with several high-impact events occurring in recent winters, notably during the 2018–2019 and 2020–2021 winters in North America (Lee and Butler, 2020; BBC; Lillo et al., 2021; Doss-Gollin et al., 2021; CNN) and the 2017–2018 winter in Europe (Kautz et al., 2020; LeMonde, 2018). Moreover, even if the absolute severity of cold spells decreases, rapid temperature swings are a hazard in their own right (Kral-O'Brien et al., 2019; Casson et al., 2019).

4.2.2 Attribution of the French Spring cold ~~spells~~ spell to climate change

A statistical analysis of the temperatures during the French cold spell of 2021 was proposed by a team of the World Weather Attribution (Vautard et al., 2021). This report concluded that while climate change has raised the absolute temperatures during cold spells, it has also led to an intensification of growing-period frosts due to earlier bud burst. The 2021 cold outbreak occurred right after a specific weather pattern called the "Atlantic Ridge", identified as one of the four main weather regimes in the North Atlantic region (Michelangeli et al., 1995). The goal of this section is to analyse how the features of this weather pattern have evolved with climate change using the ERA5 reanalyses (Figure 3). This analysis complements the report of Vautard et al. (2021) by examining the atmospheric circulation. We focus on the date of 06-04-2021, the day where the circulation particularly favored the advection of cold air into France. For this day the slp pattern (~~a) consists~~ Figure 3a) consisted of a ridge of high pressure over the Atlantic and a large cyclonic structure over Scandinavia, with cold air advection from Northern latitudes into France. The ~~analogs~~ analogues associated with this circulation in the counterfactual (Figure 3b) and factual (~~c)~~ Figure 3c) periods exhibit the same zonal pressure gradient, and their difference (Figure 3d) shows that the gradient is amplified in factual world, leading to ~~colder~~ stronger cold advection towards France. The $t2m$ for the 06-04-2021 (Figure 3e) shows cold conditions over Northern and Western Europe, while the ~~analogs~~ analogues are milder (Figure 3f,g) and $\Delta t2m$ is mostly everywhere greater than $0°C$. If we focus over France, we can conclude that this cold spell would have lead to

~~temperature 2-4~~temperatures 2–4°C colder without anthropogenic forcing. Looking at the precipitation maps (Figure 3i,j,k) and the Δtp (Figure 3l) we see that ~~this~~ the cold spell atmospheric pattern corresponds to dry conditions over continental France. There is no change ~~of~~ in precipitation patterns over France between the factual and counterfactual conditions. ~~We observe that the atmospheric conditions triggers precipitation over continental and northern Europe. The~~ However, the reinforcement of the ~~pressure gradient~~ zonal pressure gradient in the factual period leads to an increase of the precipitation over continental Europe and a decrease on the Mediterranean sea. The values of Q (Figure 3m) suggest that the pattern under examination is rare compared to its ~~analogs~~analogues, with a tendency to become even rarer in the factual period. The distribution of the predictability index D (~~n) tends to decrease~~ Figure 3n) shifts towards lower in the factual period, ~~While there are~~ although there are no significant changes relative to the counterfactual distribution. Similarly, there are not significant shifts in the persistence Θ (Figure 3o). Nonetheless, the extreme itself becomes markedly more persistent relative to the atmospheric circulation in the factual period. The monthly distribution of the ~~analogs (~~analogues (Figure 3p) suggests that there is a ~~significant~~ shift of this circulation pattern towards summer and autumn months, and that its occurrence in winter is decreasing in recent times.

Fig. 3q suggests a significant change in the ENSO phases associated with the analogues in the two periods, while no significant role of the AMO is detected with this analysis (Fig. 3r). Therefore the attribution of this event to climate change comes with the caveat of a potential role of ENSO on this pattern of atmospheric circulation.

To conclude, our analysis suggests, in line with the literature on cold spells and climate change cited in Section 4.2.1, that ~~this~~ the French Spring cold spell event is becoming ~~rare~~ rarer in the current climate and that it would have ~~lead~~ led to cooler temperatures in a world without climate change.

4.3 Westphalia floods

On July 11th, 2021 the synoptic situation over Western Europe was characterized by a ridge situated West of Ireland. As this low-pressure system ~~—~~ named “Bernd” by the German Meteorological Service (DWD, see Junghänel et al. (2021)) ~~—~~ gradually moved eastward, it was isolated from the usually westerly large-scale flow by a strong anticyclonic system that built up over the Eastern part of the Atlantic and deviated the jet stream north of Scotland. By July 13th, Bernd was completely cut from the main flow and remained stationary over Western and Central Europe until July 16th, before being gradually pushed east. Hot and moist surface air from Northern Europe and the Mediterranean was advected by the cyclonic movement around the cut-off, which led from July 12th to July 15th to recurrent and persistent heavy rains first over mountain ranges due to orographic and dynamic uplift and then over the entire region of Belgium, Luxembourg, Western Germany and Eastern France. The maximum precipitations over the region were centered on the west of Belgium with some locations receiving more than 250mm of rain in 48 hours (e.g. in Jalhay, Belgium, according to what reported by Kreienkamp et al. (2021)). The soils, already humid due to recurring precipitation events during the preceding three weeks, were incapable of absorbing more water which led to runoff and overflow of small watercourses and flash floods. Afterwards, larger rivers such as the Ruhr and the Meuse also overflowed, causing massive casualties mainly in Germany (196 people, according to DieWelt (2021)) and Belgium (42 casualties, according to Het Laatste Nieuws (2021)). In addition to the terrible fatalities, the floods severely damaged goods and infrastructures, with a total cost estimated around €10 billion (https://www.businessinsurance.com) for Belgium. It was

afterwards found using hydrological data that the flood in the regions affected was significantly higher than any flood since the beginning of the systematic records (Kreienkamp et al., 2021).

4.3.1 Floods and climate change

Rapidly after the event, the potential link between the event and climate change was highlighted by activists and journalists. Indeed, as the atmosphere warms up, it can contain more water ~~–~~ 7% per degree K of warming according to the Clausius-Clapeyron relationship ~~–~~ therefore allowing more ~~powerful~~ intense extreme precipitation events. Several studies (Madsen et al., 2014; Kundzewicz et al., 2018, 2019) investigated the link between climate variability, extreme precipitation and hydrological floods globally and in Europe. As stated in the last IPCC report (Allan et al., 2021)~~summarising scientific literature on the link between flooding events and anthropogenic climate change~~, there is high confidence that "a warmer climate will intensify very wet and very dry weather and climate events and seasons, but the location and frequency of these events depend on projected changes in regional atmospheric circulation." Especially for Europe, there is medium confidence that at 1.5°C of warming, "heavy precipitation and associated flooding are projected to intensify and be more frequent". This result highly depend on the type of water basins, especially if the peak flow is snowmelt-dominated~~, and more generallyheavy precipitation~~. More generally, heavy precipitations are strongly entangled with natural variability of the climate system. ~~In the end~~Ultimately, although flooding usually depend strongly on the local characteristics of the hydrological system ~~–~~ especially artificialization of soils and containment of rivers ~~–~~ more intense flooding can be linked to climate change via the increased intensity of heavy rains.

4.3.2 Attribution of Westphalia floods to climate change

An attribution study of the Westphalia floods has already been published by the World Weather Attribution network, who investigated the influence of climate change on heavy precipitations over a broad region of Western Europe (Kreienkamp et al., 2021). The authors of the study concluded that a climate warming of 1.2°C (current climate) led to an increase of the likelihood of such an event by a factor between 1.2 and 9 with respect to the pre-industrial period. Here~~we take an approach based on analogs of the atmospheric circulation, which allows to take into account the atmospheric~~ , we condition the attribution results on the atmospheric dynamics leading to the occurrence of ~~the event~~similar events. Results of our attribution analysis are displayed in Figure 4. We found ~~a small~~ no significant decrease in the slp of the cut-off low over Germany ~~by 2-3hPa (~~between the factual and counterfactual periods (Fig. 4a-d)~~but almost no significant changes in the 2m temperatures~~ , and only moderate increases in $t2m$ over the regions of interest (Fig. 4e-h). We found ~~, however,~~ also a large and significant increase in precipitation (up to 5mm/day) over south-west Germany, eastern France and the western Alps (Fig. 4i-l). This increase is consistent with the increasing amount of water ~~that a hotter~~ vapour that a warmer atmosphere can carry~~but can also be explained by the increased advection of most air by the stronger cut-off over Germany.~~ .

Overall, the ~~analogs quality (~~analogues quality (Fig. 4m) is good in both periods~~which reinforce our conclusions and~~ . It allows us to emphasize that, even if intense precipitation events due to cut-off lows over Western Europe in summer are not unusual, this event was particularly intense and climate change likely made it more intense ~~. While no~~ via an increased quantity

of water vapour in the atmosphere. No significant changes are observed ~~for~~ in the distributions of predictability D (~~n), the persistence index~~ Fig. 4n) and persistence Θ (~~o) is higher in the recent period, indicating that recent cut-offs are more likely to stay stationary in Western Europe, leading to longer lasting precipitation events and potentially more intense floods~~Fig. 4o), nor in the predictability or persistence of the event itself relative to the circulation in the two periods. In the factual period, events tend to happen slightly more frequently in the month of July (Fig. 4p), a favorable month for the development of large convective systems in the area~~.~~, but overall changes in seasonality are small. When investigating the link between the event and low-frequency variability of the climate system, Fig. 4q shows no significant difference in the ENSO distributions during analogue occurrences between the factual and counterfactual periods, even though the distribution in the counterfactual period is broader. Fig. 4r however displays a significant change between the AMO distributions, the analogues in the factual period being found in warmer phases of the AMO than in the counterfactual period. This suggests that attributing this event to climate change requires disentangling the possible role of AMO versus global warming.

In summary, the Westphalia floods occurred after an intense rain event caused by a cut-off lows stagnating over the region of Belgium, Luxembourg, Western Germany and Eastern France. They caused massive casualties and severely damaged goods. Our analysis is coherent with the existing literature which shows that a warmer atmosphere leads to an intensification of extreme rain events which in turn can exacerbate the intensity of floods. It should nonetheless be emphasized that attributing this event requires to take into account the role of low-frequency climate variability on the results.

4.4 Mediterranean Heatwave

During the month of August, an area of high pressure in the upper troposphere affected a large part of the Mediterranean basin. The upper lever ~~tropospheric~~ high pressure system caused ~~a downward movement in the atmosphere that~~ atmospheric subsidence which simultaneously compressed the air and warmed it, a phenomenon known as ~~heat dome.~~ "heat dome". This atmospheric configuration induced a severe heatwave over the Mediterranean region from August 10th to 15th: ~~south~~ southern Italy, France, Spain and north Africa were ~~the area mostly affectedwith wildfires and maxima temperaturesrecord. Indeed, under a high pressure system, the winds tend to be weak, so the heat does not dissipate and help to keep the conditions increasingly warmer especially with the summer sun heat.~~ most affected, with extensive wildfires and high temperatures. On August 11th, record-breaking temperatures were recorded at several locations in Italy. The town of Santa Maria Capua Vetere in Campania reached 42.2° C, 44.5° C were recorded at Bova in Calabria and 43.6° C at Ballao in Sardinia (3Bmeteo, 2021). The highest temperature was recorded in eastern Sicily with a peak of 48.8°C recorded ~~by the SIAS (2021)~~ in Floridia in the province of Syracuse (SIAS, 2021). This is the current European temperature record. ~~This value represents the highest value recorded in Italy and Europe.~~ From August 12th, the heat dome moved towards Spain. ~~The~~ There, the heat peak was reached on August 14th~~for Spain~~, establishing a new national temperature record of 47.4° C in Montoro, Andalusia ~~, as recorded by the AEMET (2021a)~~(AEMET, 2021a). The heatwave also reached ~~south-east~~ south-eastern France, where 40.9° C ~~were~~ was recorded in Varages in the Var, and 41.2° C in Trets, Bouches-du-Rhône~~(41.2° C). Same~~ . Some records were broken also in Tunisia, with 47° C in Tunis and 50.3°C in Kairouan (WMO, 2021). The heatwave ~~also triggered a large spread of~~ additionally triggered extensive wildfires in Italy, Spain, France and Greece. During the night of August 11th to 12th, more than 500 fires

were recorded in Italy, causing 4 casualties (CEMS, 2021c). Spain ~~also faced flames~~ faced fires in the area of Navalacruz and Riofrio. A fire of 90 km of perimeter devastated 12 000 hectares of vegetation and led to the evacuation of 1000 inhabitants (CEMS, 2021a). Similarly in the Var (France) wildfires burned ~~6 300~~ 6300 hectares and resulted in the evacuation of 7000 people and the death of 2 people (CEMS, 2021b).

4.4.1 Mediterranean Heatwaves and climate change

~~August is known as a hot and dry month in~~

The IPCC AR6 (Ali et al., 2022) clearly highlights the major changes in heatwave characteristics in the Mediterranean region ~~. However, the temperatures observed this summer are extreme and are typical of what is expected from~~ brought about by climate change. ~~In fact, according to the IPCC's Sixth Assessment Report AR6 (Allan et al., 2021), as a result of~~ The report states that: "Surface temperature in the Mediterranean region is now 1.5°C above the pre-industrial level, with a corresponding increase in high-temperature extreme events (high confidence)" and that "A growing number of observed impacts across the entire basin are now being attributed to climate change, ~~we are experiencing more frequent and severe high temperature events, and that this trend will continue in the future. It indicates that the frequency and intensity of heat extremes,including marine heatwaves, have increased in recent decades and are projected to continue to increase under all greenhouse gas emission scenarios.Temperatures in the Mediterranean region have increased more than the global average (Allan et al., 2021).The IPCC claimed that , for the European Mediterranean, there will be a combination of changes related to climate drivers (e. g. less precipitation and snow, changes in the sea levels mean and extremes) by mid-century and for global warming of at least 2°C and greater~~ along with major roles of other forcing of environmental change (high confidence). These impacts include multiple consequences of longer and/or more intensive heat waves,...". Finally, The report states that "During the 21st century, climate change is projected to intensify throughout the [Mediterranean] region. Air and sea temperature and their extremes (notably heat waves) are likely to continue to increase more than the global average (high confidence).~~For the North African Mediterranean, the IPCC predicts a decrease in mean precipitation and increase in fire-related weather, as well as an observed and projected increase in aridity, meteorological, hydrological, agricultural and ecological droughts (Allan et al., 2021)~~" Several studies in the literature have investigated the changes related to climatic factors in the Mediterranean, coming to similar conclusions concerning the generalised increase in heatwave frequency and intensity expected in the region (e.g. Guerreiro et al., 2018; Molina et al., 2020), and also highlighting that this may be accompanied by a drying trend (Spinoni et al., 2020; Grillakis, 2019).

4.4.2 ~~Attribution of the Mediterranean Heatwave to climate change~~

~~We use the~~

4.4.3 Attribution of the Mediterranean Heatwave to climate change

We use ERA5 ~~dates~~ to perform the attribution of the anticyclonic circulation associated with the Mediterranean heatwave in past and present ~~climate. First, we~~ climates. We note that we will select the ~~analogs~~ analogues independently of the extratropical or tropical nature of the depression that produced them. Figure 5 shows the results for the ~~heatwave over Sicily~~11-08-2021, when the heatwave peaked over southern Italy. We do not detect a significant change in the slp for the factual period compared to the counterfactual period (Figure 5 a-d). However, we ~~observe that temperatures (e-g) are significantly warmer (h)in the recent period, especially over the island and the southern~~ do observe a significant warming in $t2m$ in the factual analogues compared to the counterfactual ones (Figure 5h), with positive $\Delta t2m$ anomalies of 2 – 3°C over much of the land areas in the western Mediterranean basin. ~~This warming~~ Nonetheless, the factual analogues are still cooler that the observed extremely warm conditions on the 11-08-2021 (Figure 5e, g). The warming in the factual period is associated with a significant decrease in ~~precipitation in the factual period, especially in southern Europe~~tp in southern continental Europe and over Sicily, that could be explained by the high ~~temperature~~ temperatures and stability which suppress convection (Figure 5 i-l). ~~We detect remarkable changes in the~~ The Q values (Figure 5 m) suggest a reasonably good analogues quality in both periods. Again in both periods, the extreme event predictability index D ~~(~~is close to the maximum of the analogues distributions (Figure 5 n), ~~which~~ despite the fact that the two distributions are significantly different. This means that the slp pattern ~~tends to be more unpredictable in the present time, and we find a slight decrease in the persistence~~ for the observed heatwave was unpredictable relative to its analogues. Moreover, the event's D is higher when calculated on the factual period data than on the counterfactual period data. Persistence Θ ~~(~~shows no significant changes in the analogues' distribution, nor large changes in the event's Θ as computed from the data in the two periods (Figure 5 o). ~~Finally, we notice that the number of analogs per season is increasing in the factual period, in June and September (m).~~ Only minor changes in seasonality are observed (Figure 5 p). We finally looked at the possible influence of the low-frequency variability (ENSO and AMO) on the analogues (Figure 5q,r). We cannot dismiss the impact of ENSO and AMO variability as the distributions of both indices conditioned on the analogues change significantly between the factual and counterfactual periods. Specifically, the ENSO distribution shifts from weakly negative to neutral values, while the AMO distribution shifts from weakly negative to positive values.

In summary, our analysis is ~~perfectly~~ in line with the existing literature cited in Section 4.4.1, as it shows the ~~large~~ predominance of the thermodynamic effects of climate change on the heatwave, with a clear warming signal ~~, higher on the area than~~ in the analogues, higher than that of the global average. This signal is associated with dryer conditions over land~~and an extension of this circulation patterns towards the beginning and the end of summer~~. We nonetheless reiterate the possible influence of low-frequency climate variability on our results.

4.5 Hurricane Ida

Hurricane Ida ~~is~~ was a tropical and post-tropical cyclone ~~event that occured~~ that occurred in the North Atlantic basin (Caribbean Sea & Mainland USA) in ~~August-September~~ August 2021. Besides being the most intense TC to make landfall in the ~~US this~~ USA in that season, it had a very damaging post-tropical stage. Hurricane Ida (track shown in Figure 6) was first detected as a tropical wave on August 23th. It was named as a tropical storm on August 26th and it became a Category 1 Hurricane on the day it made a first landfall over Cuba on August 27th. This landfall did not weaken it, and it underwent rapid intensification

as it approached Louisiana's coast, were it landfell again as a Category 4 hurricane (NHC/NOAA, 2021). At its peak intensity, 1-minute sustained winds reached ~~240km~~240 km/h and the minimum central pressure was ~~929hPa~~929 hPa. Notably, it did not rapidly weakened because of the "brown ocean effect", where flat and moist land conditions allow a TC to retain its intensity for a longer period of time. Ida finally dropped below hurricane strength on August 30th.

While it was still a tropical wave, Ida triggered floods in Venezuela with 20 casualties. ~~in~~ In Cuba, the material damage was important, but no casualties were reported. In Louisiana and Mississippi there were a total of 38 deaths, among which 23 indirect, mostly for ~~CO~~ carbon monoxide poisoning (CDC, 2021). A large power outage left more than 1 million people in black-out. Heavy infrastructural damage is estimated around $15 billion (NCDC/NOAA, 2021). These figures can be compared to Katrina's — the costliest hurricane to date, that made landfall on the same date and the same place 16 years before — 1838 deaths and $125 billion damages (NHC/NOAA, 2018). ~~It shows that New Orleans was better prepared, and the forecast improved a lot as well (NHC/NOAA, 2005).~~

While Ida was ~~degenerating~~ weakening into an extratropical low, it combined with a frontal zone regaining tropical-storm force winds, and unleashing large amounts of rainfall over Northeastern ~~US. This region was much less prepared, so that the casualties were greater than the tropical stage~~USA. The casualties in this region were greater those for Ida's tropical stage, with 42 deaths ~~, mostly because of the~~ mostly due to flash floods. Finally, Ida ended its course over Eastern Canada, dissipating in the Gulf of St. Lawrence.

4.5.1 Hurricanes and climate change

~~Among~~ Of all extreme events, tropical cylones (TC) are among those for which the ~~prediction of the evolution with climate change is~~ impacts of climate change are the most uncertain. ~~This the reasons~~ The reason for this is threefold: (i) The lack of a satisfying theory for cyclogenesis, (ii) the ~~short-span~~ short span of reliable observations, and (iii) the difficulty to simulate ~~TC~~ TCs in state-of-the-art global models, because of their too coarse resolution. Despite the relatively short span of ~~observation available~~ available observations, some conclusions can still be drawn from the past record (Knutson et al., 2019). ~~Because of different trends in different regions, it is impossible to conclude on a global trend in TC frequency, but~~

Notably, the IPCC's AR6 ~~(Allan et al., 2021) note that~~ report (Allan et al., 2021) states that : "it is ~~*likely* that the global proportion of major TC occurrence has increased over the last four decades.~~ very likely that heavy precipitation events will intensify and become more frequent in most regions with additional global warming. At the global scale, extreme daily precipitation events are projected to intensify by about 7% for each 1°C of global warming (high confidence). The proportion of intense tropical cyclones (categories 4-5) and peak wind speeds of the most intense tropical cyclones are projected to increase at the global scale with increasing global warming (high confidence)." ~~Moreover, the latitude of the peak intensity shifted poleward (Kossin et al., 2014). Heavy precipitation associated with TC is also increasing with *high confidence*.~~(SPM, B2.4)

Damages have been increasing, because of a larger amount of exposed wealth, but also a decrease in TC translation speed (Kossin, 2018). ~~In the future, modeling~~ Modeling studies using different methodologies (large-scale indicators vs. direct TC tracking) disagree on the sign of ~~a~~ future global TC frequency ~~trend. But there is~~ trends. There is nonetheless some confidence in trends of TC-related risks. Knutson et al. (2020) highlight ~~consequences~~ these in order of ~~certainty: i~~decreasing certainty:

(1) because of sea-level rise, storms surges will become more important; ii(2) TC precipitation rates will increase, iii(3) The proportion of intense TC among all TC will continue to rise, and the maximum surface wind speed will increase of about 5%.

There is also growing concern about the increase in windstorm risks associated with post-tropical cyclone cyclones (Haarsma, 2021). Indeed, studies in reanalyses showed that despite representing a small number of extra-tropical storms, post-tropical cyclones are among the most intense ones to reach North America and Europe (Baker et al., 2021; Sainsbury et al., 2020). A global climate change projection show shows that more tropical cyclones are likely to undergo post-tropical transition in the future, especially in the North-Atlantic basin (Michaelis and Lackmann, 2019).

4.5.2 Attribution of Hurricane Ida to climate change

We now focus on the day Ida produced heavy precipitation in New-York city, namely the 02-09-2021, and apply the analogs analogues methodology to perform attribution. First of all, let us an attribution. We note that we will select analogs independently on select analogues independently of the extratropical or tropical nature of the depression that have has produced them. Figure 7a) shows the daily slp associated with Ida on the chosen date and (Figure 7b) and (Figure 7c) the analogs average computed analogues average for the counterfactual and the factual periods. We find a significant weakening of the slp depression (i.e. an increase of the minimum slp) for the factual with respect to the factual period (counterfactual period (Fig. 7d). Furthermore, we observe that temperatures (Fig. 7e-g) are significantly warmer (Fig. 7h) in the recent periodespecially on the sea grid-points surrounding the North-East US and Nova Scotia. This warming is associated with a significant increase of precipitation in the factual period due to the larger availability of heat and humidity (i-lfactual period. The signal of changes in analogues' precipitation between the two periods is mixed, and both sets of analogues additionally display relatively different precipitation patterns from that observed for Ida (Fig. 7i–l). We have confidence in these results because the quality of the analogs analogues Q for the event is in the bulk ofthe distribution well within (albeit in the upper tails of) the distributions of Q for its analogs analogues in both factual and counterfactual periods (Fig. 7m). We do not observe shift in The distribution of analogue quality changes significantly between the two periods, and we observe that the distribution is narrower and shifted towards lower values in the factual period, meaning that the event is becoming more typical (Fig. 7m). There is also a significant change in predictability of the analogues distribution, with a shift towards lower D (n) or in Θ (o) in the factual vs counterfactual period. Finally we do and hence higher predictability, Fig. 7n), but not in persistence (Fig. 7o). We see an increase of analogs in the month analogues in the months of August/September in the factual period (Fig. 7p): these months are at in the tropical cyclone season in the North Atlantic and therefore similar patterns could trigger deep convection in association with cyclonic depressions, leading to extreme precipitations as observed in the case of Ida. it is likely that more events in the factual period correspond to post-tropical cyclones. This is in line with the significant change in the AMO distribution between the two sets of analogues, with a shift towards more positive (warmer) values in the factual period (Fig. 7r). Indeed, a warmer phase of the AMO favors cyclonic activity and hence post-cyclonic activity. There is no significant change in the distribution of ENSO between the two sets of analogues (Fig. 7q).

Ida was already a rare extreme event as a category 4 hurricane, but it will leave a mark especially because of its impactful post-tropical stage. As we have discussed in Section 4.5.1, very intense hurricanes will are likely to become more frequent with

climate change, and they will be more likely to undergo post-tropical transition. What is particular for Ida, however, is that this transition occurred inland. What allowed the storm to remain intense in between a very strong tropical cyclone stage and the encounter with an extra-tropical perturbation could be the wet and warm ~~condition~~ conditions allowing for the "brown ocean effect". ~~Such conditions are expected to be more likely with climate change. However,~~ However, we are aware of no formal study of such inland post-tropical cyclones ~~have been made that we are aware of. While our attribution~~ in the literature. An important caveat of our analysis is that it does not take into account the ~~tropical/extratropical nature or the direction of the storm, we believe that the seasonal shift of the analogs towards late summer together with the temperature increase in the Atlantic in the factual world provides a solid explanation of the potential danger of this kind of events in the present climate~~post-tropical or extra-tropical nature of the analogue storms, but only their *slp* footprints, so that it is hard to disentangle changes in the type of events that would occur in the area, and the impact of climate change on each type of event. Our results nonetheless highlight a potential increase in autumn storm risk over north-eastern North America, and a possible AMO-driven modulation in the observed signal.

4.6 Po Valley ~~Tornadoes~~ Tornado Outbreak

On September 19, 2021, an outbreak of ~~7~~ seven tornadoes affected the Central Po Valley, in Northern Italy. In particular, ~~6~~ six of these formed in Lombardy and one, the most intense and damaging, hit a small airport near Carpi, ~~Emilia Romagna~~Emilia-Romagna. Both mesocyclonic and non-mesocyclonic vortices were observed during the event, ~~making it~~ one the most impressive tornado outbreaks on record for the region. While tornadoes and waterspouts ~~happen~~ do occur regularly in Italy, they are on average much less frequent and less intense than in ~~highly affected areas ,~~ areas such as the Mid-Western and South-Eastern ~~US~~USA. However, the structure and location of the Po Valley can lead to the insurgence of environmental conditions conducive for occasionally intense phenomena, including tornadoes reaching EF4+ intensity on the Enhanced Fujita scale (Doswell III et al., 2009). During the summer, the Po Valley can ~~be characterized by the persistence of~~ persistently host hot and humid air~~, and the~~ . The presence of the Adriatic Sea to the South-East provides an additional source of moisture, which can be advected to the region by the low-level ~~jets~~ jet preceding low pressure ~~areas~~ systems approaching from the North-West. Moreover, the presence of the ~~Appennini~~ Apennines mountain range can encourage the formation of dry lines in case of South-Westerly flow due to foehn effect, contributing to supercell development (Alberoni et al., 1996). On September 19th, a high pressure system ~~was elevated~~ extended from the Central Mediterranean Sea to Scandinavia, while a high-level low pressure was approaching the Po Valley from France, connected to a trough located over North-Western Europe. During the afternoon, the region was affected by a ~~favourable~~ dynamic and thermodynamic setup favourable to tornado development: a hot and humid low-level jet from the East, a strong wind shear with winds from the South-West at 500 hPa, a jet stream from the West at 200 hPa, and an approaching upper-level low characterized by relatively cold air, and by the entrainment of stratospheric dry air. This led to the formation of strong thunderstorms associated with ~~6~~ six tornadoes over Lombardy, roughly arranged along a line between the cities of Milan and Brescia. Around 5 pm, an isolated thunderstorm formed to the South-East of this area, closer to the ~~Appenninic~~ Apennines range, and assumed markedly supercellular features, with a hook-echo reflectivity signature, a doppler velocity couplet and a deviation to the right ~~w.r.t.~~ with respect to the mid-level flow: all clear signs of a

strong rotating updraft. This supercell produced a well-documented ~~significant~~ tornado which hit a local airport, resulting in possible EF3 damage (Poli and Stanzani, 2022).

4.6.1 Tornadoes and Climate Change

~~Past and future trends in tornado occurrence have been the object of investigation in several studies, summarised in the~~ The IPCC AR6 ~~(Allan et al., 2021). In particular, the IPCC reports that observed~~ , Chapter 11 (Seneviratne and Zhou, 2021) states that past trends in tornado occurrence are ~~associated with low confidence,~~ not robust due to short ~~time series, reporting inhomogeneity and observation bias; low confidence affects also the estimation of future trends, due to the intrinsic difficulty associated with projections of small-scale convective extremes. However, medium confidence is given to a tendency of tornadoes to be clustered in less frequent but more efficient outbreaks, characterized by a higher number of tornadoes per episode, with a total tornado number approximately constant over time. High~~ observation time series and that "There is medium confidence that the mean annual number of tornadoes in the USA has remained relatively constant, but their variability of occurrence has increased since the 1970s, particularly over the 2000s, with a decrease in the number of days per year, and an increase in the number of tornadoes on these days (high confidence). Detected tornadoes have also increased in Europe, but the trend depends on the density of observations." Moreover, even though high confidence is given to ~~the projected increase in frequency of environments conducive for the formation of tornadoes. Finally, it is concluded that attribution efforts for this phenomenon are beyond current modelling capabilities (Allan et al., 2021).~~an increase in CAPE over the tropics and subtropics; over the USA, the increase of CAPE is not associated to a decrease in the vertical wind shear. This according to the IPCC suggests "favourable conditions for an increase in severe convective storms in the future, but the interpretation of how tornadoes or hail will change is an open question because of the strong dependence on shear".

Finally, the IPCC report concludes that it is "extremely difficult to detect and attribute changes in severe convective storms." (Seneviratne and Zhou, 2021). Most studies are focused on the ~~US~~USA, pointing to an increased variability, efficiency and possibly intensity of tornado outbreaks in the last decades (Brooks et al., 2014; Elsner et al., 2015, 2019);~~however~~. However, tornadoes in Europe remain an underestimated threat (Antonescu et al., 2017), even though they can ~~interest~~ affect very densely populated areas, as in the case described in this article.

4.6.2 Attribution of the Po-Valley Tornadoes Outbreaks to climate change

~~We conclude by using the ERA5 dates to perform~~ Figure 8 shows the results for the attribution of the synoptic configuration associated with the ~~outbreak in the past and present climate.Figure 8shows the results for the episode. We find a significant but modest and unstructured increase of the *slp* field for the~~ Po Valley tornado outbreak episode. We do not observe significant differences in the pressure field over the Po Valley, and only a marginally weaker low pressure area in the Genoa Gulf (Fig. 8a-d) for the factual with respect to the counterfactual ~~period (a-d)~~analogues. Instead, we observe that temperatures ~~(e-g)~~ are significantly warmer (Fig. 8h) in the recent period, ~~both over landand the Mediterranean~~ especially over land, including the Po Valley, and the Adriatic sea. This provides an increased amount of convective potential energy, though the transport of hot and humid air within the low-level jet. ~~Precipitations associated with this configuration are higher~~ The factual period atmospheric

configuration is further associated with higher precipitation over the Alps and Central Europe, ~~while slightly lower~~ and slightly lower precipitation over the Italian peninsula (Fig. 8i-l)~~. The analogs~~ , which is coherent with a more intense transport of warm and humid air from the South-East.

The analogues quality shows that this circulation pattern is relatively common compared to the rest of the ~~analogs~~analogues. We do not detect visible changes in the predictability D (Fig. 8n) and persistence Θ (Fig. 8o) of the ~~configuration. Finally, we observe that the~~ analogues between the two periods. However the predictability of the event itself is lower (higher D) when computed using data from the factual period. The seasonal occurrence of ~~analogs (~~analogues (Fig. 8p) is quite consistent with the months of occurrence of tornadoes in ~~the country~~Northern Italy, with a maximum during summer; however, we do observe a ~~shift of the peak from August to~~ general shift towards analogues occurring earlier in the season during the factual period, with the largest increase in July, when land surface temperatures reach the annual maximum and the probability of low pressure areas entering the Mediterranean basin is higher than in May or June, offering more energy and occasions for convective instability. Finally, changes in the distributions of ENSO (Fig. 8q) and AMO between the two periods (Fig. 8r) are at the very margin of statistical significance, suggesting that no strong conclusion can be drawn on the influence or lack thereof of these modes of decadal and inter-decadal variability.

~~Concerning the impact of climate change on the occurrence of tornado outbreaks, our analysis~~ Our analysis of the Po Valley tornado outbreak shows a clear increase in temperature ~~associated to the analogs~~ of the analogues of this event in the factual period~~1992-2021~~. This is compatible with the ~~enhancement of thermodynamic setups~~ occurrence of more favourable environments for tornadoes due to climate change as mentioned in Section 4.6.1~~, leading to more favourable environments for tornadoes~~. However, the small spatio-temporal scale of the phenomenon ~~require~~ requires caution in the interpretation of the attribution results.

4.7 Medicane Apollo

When the relatively cold atmospheric air coming from polar latitudes meets the warm surface of the Mediterranean Sea, extratropical cyclones change their characteristics into near-tropical depressions. These hybrids ~~-~~ termed "medicanes" (~~crasis for Mediterranean Hurricanes) by climate scientists and meteorologists -~~ portmonteau of the words Mediterranean Hurricanes) can be very damaging because of the strong winds and the intense convective precipitations (thunderstorms) originating around the eye of the storm.

Medicane Apollo (named by a consortium of European meteorological services, see Meteoweb (2021)) formed on October 28th in the Jonian sea, offshore of Sicily, from a very active low pressure disturbance~~which was very active in the days previous the formation of the Medicane~~. This low pressure system was isolated near the Balearic islands around 22nd of October and then moved ~~on~~ to the Central Mediterranean ~~sea~~ Sea, producing self-regenerating thunderstorms in the area of Catania on the 24th of October. ~~Figure 9 displays the track of the cyclone along its life-cycle. These thunderstormsresulted in extreme~~ These thunderstorms, occurred becore the extratropical cyclones became a medicane, already resulted in extremely heavy rain and floods in Catania (>400mm rain in 48h, estimated by SIAS (2021)). Figure 9 displays the track of the cyclone along its life-cycle. During the tropical phase of Apollo, according to the latest report available, at least 10 people were

killed by the storm in Sicily, Malta, Algeria and Tunisia (jbarisk, 2021). The highest wind gusts were measured on October 29th (104km/h) and the ~~pressure minimum value was estimated to~~ minimum pressure was estimated at 999 hPa. ~~From the convective precipitations associated with Apollo, the~~ The Sicilian Meteorological service SIAS measured > 200mm ~~rain~~ convective precipitation associated with Apollo in the area of Syracuse on the same date. Apollo ~~weakened~~ started to weaken on 30th October 2021~~landfalling near Baydaand stayed inland until emerging over the Mediterranean a few hours later. Then, on 2nd of November, it dissipated off the coast of Turkey.~~ , and made landfall near Bayda, Libya, a few days later.

4.7.1 Medicanes and climate change

It is difficult to study ~~the modification of~~ trends in frequency and intensity of medicanes ~~in~~ under climate change. First of all, our knowledge of historical medicanes is very limited before the satellite era~~: their frequency is estimated~~ , and they are rare events with an estimated frequency of between 1 and 2 events per year (Cavicchia et al., 2014a). Medicanes genesis is favored when an extratropical depression gets isolated from the polar jet stream. This "cut off" becomes quasi-stationary on the Mediterranean sea and can use the large availability of heat and humidity from the sea to produce organized convection. Recent studies of medicanes ~~in~~ under climate change have therefore considered two elements: the precursors, namely the cut-off low~~that get isolated from the jet stream in the Mediterranean sea~~ , and the potential for organized convection once the first condition is met (Cavicchia et al., 2014b; Romero and Emanuel, 2017; Tous et al., 2016). On one hand, ~~there is a general consensus~~ a recent study suggests that the jet stream will shift northward (Stendel et al., 2021) and therefore cut-off ~~low will become slightly less probable~~ lows on the Mediterranean ~~sea~~Sea may become slightly less frequent. On the other hand, the Mediterranean sea is warming faster than the larger oceans, increasing the potential for convection once a depression system is present in the area. We then expect to see less medicanes but more intense ones (González-Alemán et al., 2019).

4.7.2 Attribution of Medicane Apollo to climate change

We now use the ERA5 dataset to perform the attribution of the cyclonic circulation associated with Apollo in the past and present ~~climate.First of all, let us~~ climates (Fig. 10). We note that we will select ~~analogs~~ analogues independently on the extratropical or tropical nature of the depression that have produced them. ~~Figure 10 shows the results for Apollo. We already observe that the analogs~~ The analogues average slp for both the ~~periods~~ (factual and counterfactual periods (Fig. 10b,c) do not reach slp minima comparable to that of Apollo (~~a) hinting to the uniqueness of this event~~Figure 10a), although this may partly be an effect of averaging maps with cyclones at slightly different locations. The Δslp (~~d) do not display any interesting structure. Instead~~Figure 10d) displays a weak yet significant positive anomaly over the northern part of the domain, indicating that factual analogues cyclones are less deep or southward-shifted relative to counterfactual ones. Furthermore, we observe that temperatures ~~(e-g)~~ are significantly warmer ~~(h)~~ in the factual world especially on the island of Sicily and on the southern Mediterranean basin (Figure 10e-h). This warming is associated with a significant increase of precipitation in the factual period, likely due to the larger availability of heat and humidity from the sea (Figure 10 i-l). These results must be ~~taken~~ interpreted with care because the ~~analogs quality Q>60 hPa (m)~~ analogues quality clearly shows that ~~this~~ Apollo's circulation pattern is ~~rarer~~ extremely rare compared with the rest of its ~~analogs. As in the case of Storm Filomena, Apollo~~ analogues

(Figure 10m). Apollo thus appears to be a black swan event. We do not detect remarkable changes in the ~~predictability index D (n) but we see a slightly increase in~~ distributions of the predictability index D (Figure 10n) nor the persistence Θ (~~o) which~~ Figure 10o). However, the event itself displays a lower D and higher Θ when these are computed using factual data rather than counterfactual data. This could also have contributed to enhance the persistence of precipitation on the same areas. ~~Finally we do see an increase of analogs~~ We do see a clear increase of analogues in the month of September in the factual period (Figure 10p): this is the warmest month for the Mediterranean sea, hence the most favorable for the development of deep convection in association with cyclonic depressions. This factor can greatly enhance ~~precipitations~~precipitation, especially on the mountain ranges exposed to the winds, as in the case of Apollo, for the Etna and the Peloritani mountain ranges ~~.~~ in Sicily. Finally, no significant differences in ENSO (Figure 10q) and AMO (Figure 10r) distributions conditioned to analogues have been found between the factual and counterfactual periods.

~~With respect to the general statements~~ In keeping with the general trends reported in Section 4.7.1, our analysis ~~also~~ highlights the potential intensification of precipitation associated with cyclones around the island of Sicily, supported both by higher temperatures and increased occurrence of cyclones in the month of September, the warmest for the Mediterranean sea. However, we point to the black swan nature of this storm compared to its ~~analogs~~analogues, and therefore to a careful interpretation of the attribution results obtained above.

4.8 Scandinavian cold spell

During late November 2021, Scandinavia experienced record-low temperatures for the season. On the 28th November, Nikkaluokta weather station in Sweden recorded -37,4 °C, which was the lowest November temperature recorded in the country since 1980. Other stations in northern Sweden recorded their lowest November temperatures since the 1950s (SMHI, a). Comparable records occurred in the first days of December. In Norway, the -36,7 °C recorded in Kautokeino was the lowest November reading since 2002 (SMHI, b). These frigid temperatures were part of a broader area of below-average temperatures, peaking in the last week of November and first days of December, and stretching from North-Western Russia all the way to Spain (which recorded one of the top 10 coldest November months on record (AEMET)). The cold spell impacted transports, including suspension of entire train lines (SVT) and an unusually large number of road accidents in southern Sweden (SVD).

The cold spell was associated with a large ridge forming over the North Atlantic starting from the 23rd November, and drawing cold Arctic and Siberian air over the continent. A pressure dipole with a high over Scandinavia and a low over central Europe further favoured cold air advection. The Atlantic ridge persisted until early December, after which a more zonal circulation occurred, bringing warmer airmasses over large parts of Europe.

4.8.1 Scandinavian Cold Spells and Climate Change

As discussed in Sect. 4.2.1, it is virtually certain that there has been a decrease in severity and/or frequency of cold spells in the last several decades, and the consensus is that at a global level this decrease will continue in the future. Scandinavia fits this trend, and has shown a significant decrease in wintertime cold ~~spell~~ days in recent decades (Matthes et al., 2015). In the future, the decrease in wintertime cold days is expected to be stronger than in several other European regions (Dosio, 2016), as is the

increase in yearly minimum daily-mean temperature (Bernes, 2017, p. 102).

4.8.2 Attribution of the Scandinavian Cold Spell to Climate Change

Figure 11 shows the results of our attribution analysis for the Scandinavian cold spell. The *slp* ~~analogs~~ analogues suggest that the pressure dipole over Europe seen during the cold spell is quite an unusual configuration, and that such dipole has typically become weaker ~~i~~ in the factual period (Fig. 11a–d). The weaker dipole in the ~~analogs~~ analogues during both periods corresponds to warmer ~~2-m temperatures~~ $t2m$ compared to the event, but there is ~~no evident~~ only a weak increase in the temperatures of the ~~analogs~~ analogues between the two periods over Scandinavia~~(~~. The only exceptions are the coastal areas in western and northern Norway (Fig. 11h). There is ~~instead~~ additionally a strong increase in temperatures over the Norwegian and ~~Barents seas~~ Greenland seas and north-eastern Europe, in keeping with the lower pressure to the North of Scandinavia in the factual period compared to the counterfactual period (Fig. 11d). The lack of a ~~clear warming signal is not coupled to large~~ significant warming signal across Scandinavia is coupled to modest changes in the seasonality of the ~~analogs (p), nor to notable changes~~ analogues (Fig. 11p) and in precipitation and the associated cloudiness (Fig. 11l). We hypothesise that the cold Siberian airmasses contributing to the ~~cold European~~ low Scandinavian temperatures during these events ~~have not~~ may not have warmed significantly (Cohen et al., 2013).

The quality of the ~~analogs shows a modest improvement~~ analogues is good, and shows little change when moving from the counterfactual to the ~~factul world (~~factual world (Fig. 11m), ~~and no dramatic change in the persistence~~ as does their predictability (Fig. 11n). Interestingly, the unusualeness of the *slp* dipole configuration highlighted in Fig. 11a–c thus does not translate to an unusually poor analogue quality for the event in question. The persistence Θ of the analogue patterns ~~is observed (o). There is instead a clear shift of the predictability distributiontowards lower values (n), in agreement with the long-term trend towards a decrease D in the Euro-Atlantic sector (Faranda et al., 2019a), and the arguments supporting a general increase in wintertime mid-latitude slp predictability in warmer climates (Scher and Messori, 2019). The predictability of the event itself also decreases sharply, suggesting that it is a more predictable occurrence in the context of the atmospheric variability of the factual relative to the counterfactual period .~~ shows a weak increase in the factual period, albeit with no significant change in the distribution; the persistence of the event itself computed on the factual data instead increases sharply relative to that computed on the counterfactual data (Fig. 11o). This provides an alternative hypothesis to explain the weak change in Scandinavian temperatures between the two periods, in addition to the above-discussed weak warming of Siberian airmasses. Indeed the longer persistence of the SLP pattern – and hence of the cold advection – in the factual period could partly compensate the effect of warmer air being advected over the region. The increased persistence may be compared to the findings of (Matthes et al., 2015), who find no shifts from longer to shorter cold spells in the northern high latitudes, except for a decrease in only the longest episodes.

Finally, the analogues show a significant change in ENSO distribution, with a weak shift towards more positive ENSO phases in the factual period (Fig. 11q). There is an association between positive ENSO and more severe European winters

(e.g. Fraedrich, 1990, 1994), which may provide a further explanation for the lack of significant warming in the factual period analogues. The changes in AMO distribution associated with the analogues in the two periods are inconclusive (Fig. 11r).

Based on the above, we conclude that the atmospheric configuration driving cold spells such as the November 2021 episode has not become more "unusual" with climate change, and that the intensity of the cold spells engendered by similar atmospheric configurations has not weakened significantly, contrary to the decreasing trends observed in data and model simulations for cold days in Scandinavia 4.8.1. ~~As such, the~~ ENSO may provide some modulation of the cold spells characteristics between the two periods, but based on the moderate changes observed in its association with the cold spell analogues, we deem it unlikely to be the main physical driver of our results. We thus interpret the November 2021 event ~~may be seen~~ as a persistent cold extreme in a warming climate.

5 Conclusions

We have analyzed the atmospheric circulation associated with a selection of high-impact extreme events occurring in 2021 from an attribution perspective. Specifically, we have performed a semi-objective selection of a representative ~~day~~ circulation pattern for each extreme, and have then identified two sets of ~~analogs~~analogues. The first in the 1950–1979 period, which approximates a counterfactual world; the second in the 1992–2021 period, which approximates a factual world. Regardless the specificity of each event, our analysis ~~allows us to draw some conclusions that may be of relevance to the~~ evidences the relevant role of atmospheric circulation changes under anthropogenic climate change in controlling the characteristics of many of these events, which is a conclusion of relevance to the broader field of ~~extreme event attribution. First, many circulation patterns leading to extremes occur preferentially during a specific season, but are observed with lower frequency during all seasons (e.g. see the attribution of Filomena winter storm or the French spring cold spell). For many events, we have been able to identify seasonal shifts in the occurrence of event analogs with major implications for their surface impacts (e.g. see the attributionof the Scandinavian cold spell). This can occur independently of large changes in the analogue circulation patterns or the thermodynamic effect of global mean surface warming.~~ extreme event attribution.

A second important outcome of this study is to include, in the attribution framework, the systematic use of the dynamical indicators of persistence and predictability. Persistence is of particular interest, since there has been a lively scientific debate on changes in atmospheric persistence and how ~~this~~ these may affect extreme events (Coumou and Rahmstorf, 2012; Hoskins and Woollings, 2015; Wehrli et al., 2020).

Finally, we have studied the quality of the ~~analogs,~~ analogues – namely the "typicality" of the ~~analogs~~ analogues relative to the atmospheric variability – and their changes over time. This brings a third relevant outcome, namely the ability to understand whether both a given circulation and its ~~analogs~~ analogues are becoming more or less "typical" (i.e. have better or worse ~~analogs~~analogues). The two do not always vary in tandem, meaning that the quality of the ~~analogs~~ analogues for a given extreme may remain unchanged while the ~~analogs of the analogs~~ analogues of the analogues become better. While not immediate to interpret, this provides some subtle insights into how the configurations conducive to an extreme relate to the broader atmospheric variability typical of a given climate. In the case of ~~the storm Filomena and the~~ medicane Apollo, the lack of

~~analogs of good quality~~ good-quality analogues directly points to the ~~emergence~~ unprecedented nature of this event~~as an unprecedented one,~~ , making it a black swan among the weather patterns in Europe. ~~This warns that weather extreme events can appear without belonging to an existing population.~~ It is therefore questionable to attempt any attribution statements in this case. This finding is also a warning that weather extreme events do not necessarily belong to the sample of weather situations observed in the last several decades.

The main limitations of our framework include the somewhat arbitrary ~~choices~~ choice of the region used to define the ~~analogs~~analogues, the time scale for the selection of the ~~analogs and of~~ analogues and the number of ~~analogs.~~ analogues retained for analysis. Moreover, only for two of the events — the Po Valley tornado outbreak and medicane Apollo — is it possible to statistically exclude a role of natural inter-decadal variability of ENSO and AMO in explaining differences in the analogues. We are well aware of these limitations, and have designed the study to minimise their impact. The main advantage of working with ~~analogs~~ analogues of sea-level pressure is the possibility of applying expert judgement to select a region that includes the large-scale cyclonic/anticyclonic structures concurring ~~with~~ to the event. The use of daily ~~averages~~ means allows to average out the daily cycle. Longer time scales have been tested but they produce worse ~~analogs~~ analogues due to the fact that the synoptic structures move too much and lead to aliased atmospheric patterns. ~~Furthermore,~~ We nonetheless believe that longer time scales could be used to study long-lasting extreme events such as droughts. Furthermore, at daily time resolution information about the ~~eventual stationarity~~ stationarity or lack thereof of the patterns is retained in the persistence ~~metrics. Finally we~~ metric. We have tested the dependence of our results on the number of ~~analogs used~~analogues used, and found that ~~an optimum performance is reached~~ numbers between 30 and 60 ~~analogs, i.e. a number sufficiently high to have a meaningful statistics but low enough to have authentic analogs. A metric of quality of analogs has been added to control the outcome of the analogs search. Finally~~analogues provide a good balance between having meaningful statistics and selecting good-quality analogues. Finally, we highlight that conventional extreme value attribution shares many of the same limitations, including the choice of the region, thresholds and time scale.

Our approach does not want to substitute extreme ~~value~~ event attributions based on the statistical fitting of extreme value distributions: those approaches can be used to ~~provide an immediate answers to stakeholders in changes of~~ inform stakeholders of changes in return times of extreme events in factual versus counterfactual worlds, and have been successfully used by the attribution community in a large number of instances (Trenberth et al., 2015; Van Oldenborgh and Van Ulden, 2003; Vautard and Yiou, 2012; Van Oldenborgh et al., 2012; Trenberth et al., 2015; Vautard et al., 2016, 2018). We rather see our analysis as complementing statistical approaches by providing insights on the possible changes over time of the dynamics underlying ~~an extreme eventsfrom a dynamical perspective~~specific extreme events, on the line described by on Extreme Weather Events and Attribution (2 . Further development of this methodology can include the use of ~~analogs~~ analogues to flag population of events that share the same dynamical origin, on the line of research proposed by Jézéquel et al. (2018b) and Shepherd (2019). This would allow to ~~perform an attribution conditioned to the analogs and the release of~~ use the tools of statistical attribution with an additional conditioning from the analogues and to release an automated package that produces these analyses in a matter of minutes as soon as the ERA5 data are available. Other possible extensions include searching for ~~analogs~~ analogues of different observables such as geopotential height, temperature on pressure levels, winds and more. Although valuable, these options must be evalu-

ated with extreme care in the context of attribution because of the non-linear trends already introduced by the anthropogenic forcing on the average of these quantities (Jézéquel et al., 2018a).

To conclude, the ~~analogs~~ analogues approach to extreme event attribution shows that many extreme events are significantly modified in the present climate with respect to the past, because of changes in the position, persistence and seasonality of cyclonic/anticyclonic patterns. Our approach, complementary to the statistical methods already available in the attribution community, underscore the importance of considering changes in the atmospheric circulation when performing attribution studies.

Code availability. The code to compute the dynamical indicators of predictability D and persistence θ is available at https://fr.mathworks.com/matlabcentral/fileexchange/95768-attractor-local-dimension-and-local-persistence-computation

Data availability. ERA5 is the latest climate reanalysis being produced by ECMWF as part of implementing the EU- funded Copernicus Climate Change Service (C3S), providing hourly data on atmospheric, land-surface and sea-state parameters together with estimates of uncertainty from 1979 to present day. ERA5 data are available on the C3S Climate Data Store on regular latitude-longitude grids at 0.25° x 0.25° resolution at https://cds.climate.copernicus.eu/#!/home, accessed on 2022-01-26

Appendix A: Predictability and Persistence Indices

The attractor of a dynamical system is a geometric object defined in the space hosting all the possible states of the system (phase-space). Each point ζ on the attractor can be characterized by two dynamical indicators: the local dimension D, which indicates the number of degrees of freedom active locally around ζ, and the persistence Θ, a measure of the mean residence time of the system around ζ (Faranda et al., 2017a). To determine D, we exploit recent results from the application of extreme value theory to Poincaré recurrences in dynamical systems. This approach considers long trajectories of a system — in our case successions of daily SLP latitude–longitude maps — corresponding to a sequence of states on the attractor. For a given point ζ in phase space (e.g., a given SLP map), we compute the probability that the system returns within a ball of radius ϵ centered on the point ζ. The Freitas et al. (2010) theorem, modified by Lucarini et al. (2012), states that logarithmic returns:

$$g(x(t)) = -\log(\text{dist}(x(t),\zeta)) \tag{A1}$$

yield a probability distribution such that:

$$\Pr(z > s(q)) \simeq \exp\left[-\vartheta(\zeta)\left(\frac{z-\mu(\zeta)}{\sigma(\zeta)}\right)\right] \tag{A2}$$

where $z = g(x(t))$ and s is a high threshold associated to a quantile q of the series $g(x(t))$. Requiring that the orbit falls within a ball of radius ϵ around the point ζ is equivalent to asking that the series $g(x(t))$ is over the threshold s; therefore, the ball radius ϵ is simply $e^{-s(q)}$. The resulting distribution is the exponential member of the Generalized Pareto Distribution family. The parameters μ and σ, namely the location and the scale parameter of the distribution, depend on the point ζ in phase space. $\mu(\zeta)$ corresponds to the threshold $s(q)$ while the local dimension ~~$d(\zeta)$~~ $D(\zeta)$ can be obtained via the relation $\sigma = 1/D(\zeta)$. This is the metric of predictability introduced in Sect. 3.

When $x(t)$ contains all the variables of the system, the estimation of D based on extreme value theory has a number of advantages over traditional methods (e.g. the box counting algorithm (Liebovitch and Toth, 1989; Sarkar and Chaudhuri, 1994)). First, it does not require to estimate the volume of different sets in scale-space: the selection of $s(q)$ based on the quantile provides a selection of different scales s which depends on the recurrence rate around the point ζ. Moreover, it does not require the a priori selection of the maximum embedding dimension as the observable g is always a univariate time-series.

The persistence of the state ζ is measured via the extremal index $0 < \vartheta(\zeta) < 1$, an adimensional parameter, from which we extract $\Theta(\zeta) = \Delta t/\vartheta(\zeta)$. Here, Δt is the timestep of the dataset being analysed. $\Theta(\zeta)$ is therefore the average residence time of trajectories around ζ, namely the metric of persistence introduced in Sect. 3, and it has unit of a time (in this study days). If ζ is a fixed point of the attractor, then $\Theta(\zeta) = \infty$. For a trajectory that leaves the neighborhood of ζ at the next time iteration, $\Theta = 1$. To estimate ϑ, we adopt the Süveges estimator (Süveges, 2007). For further details on the the extremal index, see ~~Lucarini et al. (2016a)~~Moloney et al. (2019).

Author contributions. D Faranda conceived the study, performed the attribution analysis for all events and wrote the section on the medicane Apollo. S Bourdin wrote the section on Hurricane Ida and performed cyclone tracking analyses. M Ginesta wrote the section about storm Filomena. M Krouma wrote the section about the Mediterranean Heatwave. R Noyelle wrote the section about the Westphalia floods. Flavio Pons wrote the section about the Po Valley tornadoes outbreak. Pascal Yiou wrote the section about the French spring cold-spell. G Messori wrote the section about the Scandinavian Cold Spell and contributed to the final drafting of the manuscript. All the authors contributed to writing and reviewing the introduction, methods and conclusion of the article.

Competing interests. The authors declare no competing interests

Acknowledgements. The ~~author wishes~~ authors wishe to thank MC Alvarez-Castro, J Riboldi, M Galfi, M Vrac, A Hisi, E Coppola~~and R Vautard for the discussions~~, R Vautard and two anonymous reviewers for useful discussions and inputs. The authors acknowledge the support of the INSU-CNRS-LEFE-MANU grant (project DINCLIC), ~~as well as the gran~~ the grant ANR-19-ERC7-0003 (BOREAS) and the grant ANR-20-CE01-0008-01 (SAMPRACE). This work has received support from the European Union's Horizon 2020 research and innovation programme under grant agreement No. 101003469 (XAIDA), by the European Research Council (ERC) under grant agreement No. 948309 (CENÆ), and by the Marie Sklodowska-Curie grant agreement No. 956396 (EDIPI).

References

3Bmeteo: Caldo Storico in Sicilia, https://www.3bmeteo.com/giornale-meteo/cronaca-meteo---caldo-storico-in-sicilia--raggiunti-i-49-c----il-nuovo-record-europeo-504610, accessed: 2022-01-31, 2021.

AEMET: Spanish State Meteorological Agency: Noviembre de 2021, un mes muy frío, https://www.aemet.es/es/noticias/2021/12/resumen_clima_noviembre_2021, accessed: 2022-01-14.

AEMET: Spanish State Meteorological Agency, https://aemetblog.es/2021/08/18/la-ola-de-calor-del-puente-de-agosto21-y-los-records-de-temperaturas-en-espana/, accessed: 2022-01-27, 2021a.

AEMET: Spanish State Meteorological Agency: Informe sobre la borrasca Filomena y la ola de frio, http://www.aemet.es/documentos/es/conocermas/recursos_en_linea/publicaciones_y_estudios/estudios/Informe_episodio_filomena.pdf, accessed: 2021, 2021b.

Alberoni, P., Nanni, S., Crespi, M., and Monai, M.: The supercell thunderstorm on 8 June 1990: mesoscale analysis and radar observations, Meteorology and Atmospheric Physics, 58, 123–138, 1996.

Ali, E., Cramer, W., Carnicer, J., Georgopoulou, E., Hilmi, N., Cozannet, G. L., and P. Lionello, P.: Cross-Chapter Paper 4: Mediterranean Region. In: Climate Change 2022: Impacts, Adaptation and Vulnerability., Contribution of Working Group II to the Sixth Assessment Report of the Intergovernmental Panel on Climate Change, pp. 2233–2272, https://doi.org/10.1017/9781009325844.021, 2022.

Allan, R. P., Hawkins, E., Bellouin, N., and Collins, B.: IPCC, 2021: Summary for Policymakers, 2021.

Anderson, T. W.: On the distribution of the two-sample Cramer-von Mises criterion, The Annals of Mathematical Statistics, pp. 1148–1159, 1962.

Antonescu, B., Schultz, D. M., Holzer, A., and Groenemeijer, P.: Tornadoes in Europe: An underestimated threat, Bulletin of the American Meteorological Society, 98, 713–728, 2017.

Aon: Global Catastrophe Recap, http://thoughtleadership.aon.com/documents/20210209_analytics-if-january-global-recap.pdf, accessed: January 2021, 2021.

Baker, A. J., Hodges, K. I., Schiemann, R. K., and Vidale, P. L.: Historical variability and lifecycles of North Atlantic midlatitude cyclones originating in the tropics, Journal of Geophysical Research: Atmospheres, 126, e2020JD033 924, 2021.

Bala, G., Caldeira, K., and Nemani, R.: Fast versus slow response in climate change: implications for the global hydrological cycle, Climate dynamics, 35, 423–434, 2010.

BBC: Polar vortex death toll rises to 21 as US cold snap continues, https://www.bbc.com/news/world-us-canada-47088684, accessed: 2022-01-14.

Berkovic, S. and Raveh-Rubin, S.: Persistent warm and dry extremes over the eastern Mediterranean during winter: The role of North Atlantic blocking and central Mediterranean cyclones, Quarterly Journal of the Royal Meteorological Society, 148, 2384–2409, 2022.

Bernes, C.: En varmare värld: Växthuseffekten och klimatets förändringar-Tredje upplagan, 2017.

Blackport, R. and Screen, J. A.: Weakened evidence for mid-latitude impacts of Arctic warming, Nature Climate Change, 10, 1065–1066, 2020.

Brooks, H. E., Carbin, G. W., and Marsh, P. T.: Increased variability of tornado occurrence in the United States, Science, 346, 349–352, 2014.

Casson, N., Contosta, A., Burakowski, E., Campbell, J., Crandall, M., Creed, I., Eimers, M., Garlick, S., Lutz, D., Morison, M., et al.: Winter weather whiplash: Impacts of meteorological events misaligned with natural and human Systems in Seasonally Snow-Covered Regions, Earth's Future, 7, 1434–1450, 2019.

Cavicchia, L., von Storch, H., and Gualdi, S.: A long-term climatology of medicanes, Climate dynamics, 43, 1183–1195, 2014a.

Cavicchia, L., von Storch, H., and Gualdi, S.: Mediterranean tropical-like cyclones in present and future climate, Journal of Climate, 27, 7493–7501, 2014b.

CDC: Deaths Related to Hurricane Ida, https://www.cdc.gov/mmwr/volumes/70/wr/mm7039a3.htm, accessed: 2022-01-31, 2021.

CEMS: COPERNICUS Emergency Management Service, https://emergency.copernicus.eu/mapping/list-of-components/EMSR538, accessed: 2022-01-31, 2021a.

CEMS: COPERNICUS Emergency Management Service, https://emergency.copernicus.eu/mapping/list-of-components/EMSR541, accessed: 2022-01-31, 2021b.

CEMS: COPERNICUS Emergency Management Service, https://emergency.copernicus.eu/mapping/ems/copernicus-emergency-management-service-monitors-fire-events-mediterranean-region, accessed: 2022-01-31, 2021c.

CNN: These US cities had the coldest morning in decades – with some reaching all-time record lows, https://edition.cnn.com/2021/02/16/us/record-cold-weather-us-trnd/index.html, accessed: 2022-01-14.

Cohen, J., Jones, J., Furtado, J. C., and Tziperman, E.: Warm Arctic, cold continents: A common pattern related to Arctic sea ice melt, snow advance, and extreme winter weather, Oceanography, 26, 150–160, 2013.

Cohen, J., Zhang, X., Francis, J., Jung, T., Kwok, R., Overland, J., Tayler, P. C., Lee, S., Laliberte, F., and Feldstein, S.: Arctic change and possible influence on mid-latitude climate and weather: a US CLIVAR White Paper, US CLIVAR, 2018.

Coumou, D. and Rahmstorf, S.: A decade of weather extremes, Nature climate change, 2, 491–496, 2012.

D'errico, M., Yiou, P., Nardini, C., Lunkeit, F., and Faranda, D.: Warmer Mediterranean temperatures do not decrease snowy cold spell intensity over Italy, https://hal.archives-ouvertes.fr/hal-02367559/document, 2019.

DieWelt: "Hochwasser aktuell: Zahl der Toten in Rheinland-Pfalz steigt auf 135 - Mindestens 184 Opfer durch Flut in Deutschland", https://www.welt.de/vermischtes/live232509543/Hochwasser-aktuell-Mindestens-177-Opfer-durch-Flut-in-Deutschland.html, accessed: 2021-07-22, 2021.

Dosio, A.: Projections of climate change indices of temperature and precipitation from an ensemble of bias-adjusted high-resolution EURO-CORDEX regional climate models, Journal of Geophysical Research: Atmospheres, 121, 5488–5511, 2016.

Doss-Gollin, J., Farnham, D. J., Lall, U., and Modi, V.: How unprecedented was the February 2021 Texas cold snap?, Environmental Research Letters, 16, 064 056, 2021.

Doswell III, C. A., Brooks, H. E., and Dotzek, N.: On the implementation of the enhanced Fujita scale in the USA, Atmospheric Research, 93, 554–563, 2009.

Easterling, D. R., Kunkel, K. E., Wehner, M. F., and Sun, L.: Detection and attribution of climate extremes in the observed record, Weather and Climate Extremes, 11, 17–27, 2016.

Elsner, J. B., Elsner, S. C., and Jagger, T. H.: The increasing efficiency of tornado days in the United States, Climate Dynamics, 45, 651–659, 2015.

Elsner, J. B., Fricker, T., and Schroder, Z.: Increasingly powerful tornadoes in the United States, Geophysical Research Letters, 46, 392–398, 2019.

Faranda, D.: An attempt to explain recent trends in European snowfall extremes, Weather Clim. Dynam. Discuss., 2019, 1–20, https://doi.org/10.5194/wcd-2019-15, 2019.

Faranda, D., Messori, G., and Yiou, P.: Dynamical proxies of North Atlantic predictability and extremes, Scientific reports, 7, 41 278, 2017a.

Faranda, D., Messori, G., and Yiou, P.: Dynamical proxies of North Atlantic predictability and extremes, Scientific reports, 7, 41 278, https://www.nature.com/articles/srep41278.pdf, 2017b.

Faranda, D., Alvarez-Castro, M. C., Messori, G., Rodrigues, D., and Yiou, P.: The hammam effect or how a warm ocean enhances large scale atmospheric predictability, Nature communications, 10, 1–7, 2019a.

Faranda, D., Messori, G., and Vannitsem, S.: Attractor dimension of time-averaged climate observables: insights from a low-order ocean-atmosphere model, Tellus A: Dynamic Meteorology and Oceanography, 71, 1–11, 2019b.

Faranda, D., Vrac, M., Yiou, P., Jézéquel, A., and Thao, S.: Changes in future synoptic circulation patterns: consequences for extreme event attribution, Geophys. Res. Lett., 47, e2020GL088 002, iSBN: 0094-8276 Publisher: Wiley Online Library, 2020.

Flannigan, M. D., Stocks, B. J., and Wotton, B. M.: Climate change and forest fires, Science of the total environment, 262, 221–229, 2000.

Fraedrich, K.: European grosswetter during the warm and cold extremes of the El Niñco/Southern Oscillation, International Journal of Climatology, 10, 21–31, 1990.

Fraedrich, K.: An ENSO impact on Europe?, Tellus A, 46, 541–552, 1994.

Freitas, A. C. M., Freitas, J. M., and Todd, M.: Hitting time statistics and extreme value theory, Probability Theory and Related Fields, 147, 675–710, 2010.

Freitas, A. C. M., Freitas, J. M., and Todd, M.: Extreme value laws in dynamical systems for non-smooth observations, Journal of Statistical Physics, 142, 108–126, 2011.

Freitas, A. C. M., Freitas, J. M., and Vaienti, S.: Extreme Value Laws for sequences of intermittent maps, arXiv preprint arXiv:1605.06287, 2016.

González-Alemán, J. J., Pascale, S., Gutierrez-Fernandez, J., Murakami, H., Gaertner, M. A., and Vecchi, G. A.: Potential increase in hazard from Mediterranean hurricane activity with global warming, Geophysical Research Letters, 46, 1754–1764, 2019.

Gordon, L. J., Steffen, W., Jönsson, B. F., Folke, C., Falkenmark, M., and Johannessen, Å.: Human modification of global water vapor flows from the land surface, Proceedings of the National Academy of Sciences, 102, 7612–7617, 2005.

Grillakis, M. G.: Increase in severe and extreme soil moisture droughts for Europe under climate change, Science of The Total Environment, 660, 1245–1255, 2019.

Guerreiro, S. B., Dawson, R. J., Kilsby, C., Lewis, E., and Ford, A.: Future heat-waves, droughts and floods in 571 European cities, Environmental Research Letters, 13, 034 009, https://doi.org/10.1088/1748-9326/aaaad3, 2018.

Haarsma, R.: European Windstorm Risk of Post-Tropical Cyclones and the Impact of Climate Change, Geophysical Research Letters, 48, e2020GL091 483, 2021.

Hersbach, H., Bell, B., Berrisford, P., Hirahara, S., Horányi, A., Muñoz-Sabater, J., Nicolas, J., Peubey, C., Radu, R., and Schepers, D.: The ERA5 global reanalysis, Quat. J. Roy. Met. Soc., 146, 1999–2049, iSBN: 0035-9009 Publisher: Wiley Online Library, 2020.

Het Laatste Nieuws: "Een van de twee laatste vermiste personen na overstromingen in ons land teruggevonden", https://www.hln.be/binnenland/een-van-de-twee-laatste-vermiste-personen-na-overstromingen-in-ons-land-teruggevonden~a4a4c681/, accessed: 2021-07-29, 2021.

Hochman, A., Alpert, P., Harpaz, T., Saaroni, H., and Messori, G.: A new dynamical systems perspective on atmospheric predictability: Eastern Mediterranean weather regimes as a case study, Science advances, 5, eaau0936, 2019.

Horton, R. M., Mankin, J. S., Lesk, C., Coffel, E., and Raymond, C.: A review of recent advances in research on extreme heat events, Current Climate Change Reports, 2, 242–259, 2016.

Hoskins, B. and Woollings, T.: Persistent extratropical regimes and climate extremes, Current Climate Change Reports, 1, 115–124, 2015.

https://www.businessinsurance.com: "Recent floods cause nearly $12 billion damage in Belgium", https://www.businessinsurance.com/article/00010101/STORY/912343432/Recent-floods-cause-nearly-\protect\T1\textdollar12-billion-damage-in-Belgium, accessed: 2022-01-27.

Hu, S., Zhang, W., Turner, A. G., and Sun, J.: How does El Niño-Southern Oscillation affect winter fog frequency over eastern China?, Climate Dynamics, 54, 1043–1056, 2020.

Huang, B., Thorne, P. W., Banzon, V. F., Boyer, T., Chepurin, G., Lawrimore, J. H., Menne, M. J., Smith, T. M., Vose, R. S., and Zhang, H.-M.: Extended reconstructed sea surface temperature, version 5 (ERSSTv5): upgrades, validations, and intercomparisons, Journal of Climate, 30, 8179–8205, 2017.

jbarisk: Hurricane-like storm causes flooding in the Mediterranean, October 2021, https://www.jbarisk.com/flood-services/event-response/medicane-apollo, accessed: 2022-02-01, 2021.

Jézéquel, A., Dépoues, V., Guillemot, H., Trolliet, M., Vanderlinden, J.-P., and Yiou, P.: Behind the veil of extreme event attribution, Climatic Change, 149, 367–383, 2018.

Jolly, E., D'Andrea, F., Rivière, G., and Fromang, S.: Linking warm Arctic winters, Rossby waves and Cold Spells: an idealized numerical study, Journal of the Atmospheric Sciences, 2021.

Junghänel, T., Bissolli, P., Daßler, J., Fleckenstein, R., Imbery, F., Janssen, W., Kaspar, F., Lengfeld, K., Leppelt, T., Rauthe, M., et al.: Hydro-klimatologische Einordnung der Stark-und Dauerniederschläge in Teilen Deutschlands im Zusammenhang mit dem Tiefdruckgebiet „Bernd "vom 12. bis 19. Juli 2021, Deutscher Wetterdienst, 2021.

Jézéquel, A., Cattiaux, J., Naveau, P., Radanovics, S., Ribes, A., Vautard, R., Vrac, M., and Yiou, P.: Trends of atmospheric circulation during singular hot days in Europe, Environmental Research Letters, 13, 054 007, https://iopscience.iop.org/article/10.1088/1748-9326/aab5da/pdf, 2018a.

Jézéquel, A., Dépoues, V., Guillemot, H., Trolliet, M., Vanderlinden, J.-P., and Yiou, P.: Behind the veil of extreme event attribution, Climatic Change, https://doi.org/https://doi-org.insu.bib.cnrs.fr/10.1007/s10584-018-2252-9, 2018b.

Kautz, L.-A., Polichtchouk, I., Birner, T., Garny, H., and Pinto, J. G.: Enhanced extended-range predictability of the 2018 late-winter Eurasian cold spell due to the stratosphere, Quarterly Journal of the Royal Meteorological Society, 146, 1040–1055, 2020.

Kennedy, D., Parker, T., Woollings, T., Harvey, B., and Shaffrey, L.: The response of high-impact blocking weather systems to climate change, Geophysical Research Letters, 43, 7250–7258, 2016.

Knapp, K. R., Kruk, M. C., Levinson, D. H., Diamond, H. J., and Neumann, C. J.: The international best track archive for climate stewardship (IBTrACS) unifying tropical cyclone data, Bulletin of the American Meteorological Society, 91, 363–376, 2010.

Knapp, Kenneth R et al.: International Best Track Archive for Climate Stewardship (IBTrACS) Project, Version 4., https://doi.org/10.25921/82ty-9e16, accessed: 2022-01-26, 2018.

Knutson, T., Kossin, J., Mears, C., Perlwitz, J., and Wehner, M.: Detection and attribution of climate change, 2017.

Knutson, T., Camargo, S. J., Chan, J. C., Emanuel, K., Ho, C.-H., Kossin, J., Mohapatra, M., Satoh, M., Sugi, M., Walsh, K., et al.: Tropical cyclones and climate change assessment: Part I: Detection and attribution, Bulletin of the American Meteorological Society, 100, 1987–2007, 2019.

Knutson, T., Camargo, S. J., Chan, J. C., Emanuel, K., Ho, C.-H., Kossin, J., Mohapatra, M., Satoh, M., Sugi, M., Walsh, K., et al.: Tropical cyclones and climate change assessment: Part II: Projected response to anthropogenic warming, Bulletin of the American Meteorological Society, 101, E303–E322, 2020.

Kodra, E., Steinhaeuser, K., and Ganguly, A. R.: Persisting cold extremes under 21st-century warming scenarios, Geophysical research letters, 38, 2011.

Kornhuber, K. and Tamarin-Brodsky, T.: Future changes in Northern Hemisphere summer weather persistence linked to projected Arctic warming, Geophysical Research Letters, 48, e2020GL091 603, 2021.

Kossin, J. P.: A global slowdown of tropical-cyclone translation speed, Nature, 558, 104–107, 2018.

Kossin, J. P., Emanuel, K. A., and Vecchi, G. A.: The poleward migration of the location of tropical cyclone maximum intensity, Nature, 509, 349–352, 2014.

Kral-O'Brien, K. C., O'Brien, P. L., and Harmon, J. P.: Need for false spring research in the Northern Great Plains, USA, Agricultural & Environmental Letters, 4, 190 025, 2019.

Kreienkamp, F., Philip, S. Y., Tradowsky, J. S., Kew, S. F., Lorenz, P., Arrighi, J., Belleflamme, A., Bettmann, T., Caluwaerts, S., Chan, S. C., et al.: Rapid attribution of heavy rainfall events leading to the severe flooding in Western Europe during July 2021, 2021.

Kundzewicz, Z. W., Pińskwar, I., and Brakenridge, G. R.: Changes in river flood hazard in Europe: a review, Hydrology research, 49, 294–302, 2018.

Kundzewicz, Z. W., Szwed, M., and Pińskwar, I.: Climate variability and floods—A global review, Water, 11, 1399, 2019.

LaChaineMeteo: Bilan climatique d'avril 2021 : entre sécheresse et records de froid, https://actualite.lachainemeteo.com/actualite-meteo/2021-05-05/bilan-climatique-d-avril-2021-entre-secheresse-et-records-de-froid-59270, accessed: 2022-02-01, 2021.

Lee, J.-Y., Marotzke, J., Bala, G., Cao, L., Corti, S., Dunne, J., Engelbrecht, F., Fischer, E., Fyfe, J., Jones, C., Maycock, A., Mutemi, J., Ndiaye, O., Panickal, S., , and Zhou, T.: Future Global Climate: Scenario-Based Projections and Near-Term Information. In Climate Change 2021: The Physical Science Basis. Contribution of Working Group I to the Sixth Assessment Report of the Intergovernmental Panel on Climate Change, 2021.

Lee, S. H. and Butler, A. H.: The 2018–2019 Arctic stratospheric polar vortex, Weather, 75, 52–57, 2020.

LeMonde: La vague de froid se poursuit en Europe et fait des dizaines de morts, https://www.lemonde.fr/climat/article/2018/02/28/la-vague-de-froid-se-poursuit-en-europe-et-fait-des-dizaines-de-morts_5263856_1652612.html, accessed: 2022-01-14, 2018.

Liebovitch, L. S. and Toth, T.: A fast algorithm to determine fractal dimensions by box counting, physics Letters A, 141, 386–390, 1989.

Lillo, S. P., Cavallo, S. M., Parsons, D. B., and Riedel, C.: The Role of a Tropopause Polar Vortex in the Generation of the January 2019 Extreme Arctic Outbreak, Journal of the Atmospheric Sciences, 78, 2801–2821, 2021.

Lucarini, V., Faranda, D., and Wouters, J.: Universal behaviour of extreme value statistics for selected observables of dynamical systems, Journal of statistical physics, 147, 63–73, 2012.

Lucarini, V., Faranda, D., de Freitas, J. M. M., Holland, M., Kuna, T., Nicol, M., Todd, M., Vaienti, S., et al.: Extremes and recurrence in dynamical systems, John Wiley & Sons, 2016a.

Lucarini, V., Faranda, D., Freitas, A. C. M., Freitas, J. M., Holland, M., Kuna, T., Nicol, M., Todd, M., and Vaienti, S.: Extremes and recurrence in dynamical systems, John Wiley & Sons, 2016b.

Madsen, H., Lawrence, D., Lang, M., Martinkova, M., and Kjeldsen, T.: Review of trend analysis and climate change projections of extreme precipitation and floods in Europe, Journal of Hydrology, 519, 3634–3650, 2014.

Matthes, H., Rinke, A., and Dethloff, K.: Recent changes in Arctic temperature extremes: warm and cold spells during winter and summer, Environmental Research Letters, 10, 114 020, 2015.

Messori, G., Caballero, R., and Faranda, D.: A dynamical systems approach to studying midlatitude weather extremes, Geophysical Research Letters, 44, 3346–3354, 2017.

Meteoweb: Medicane Apollo, Aeronautica: per la prima volta un consorzio di Paesi europei ha dato un nome ufficiale ad un evento meteorologico, https://www.meteoweb.eu/2021/10/medicane-apollo-per-la-prima-volta-un-nome-ufficiale/1734332/, accessed: 2022-01-27, 2021.

Michaelis, A. C. and Lackmann, G. M.: Climatological changes in the extratropical transition of tropical cyclones in high-resolution global simulations, Journal of Climate, 32, 8733–8753, 2019.

Michelangeli, P.-A., Vautard, R., and Legras, B.: Weather regimes: Recurrence and quasi stationarity, Journal of the atmospheric sciences, 52, 1237–1256, 1995.

Mitchell, D., Heaviside, C., Vardoulakis, S., Huntingford, C., Masato, G., Guillod, B. P., Frumhoff, P., Bowery, A., Wallom, D., and Allen, M.: Attributing human mortality during extreme heat waves to anthropogenic climate change, Environmental Research Letters, 11, 074 006, 2016.

Molina, M., Sánchez, E., and Gutiérrez, C.: Future heat waves over the Mediterranean from an Euro-CORDEX regional climate model ensemble, Scientific reports, 10, 1–10, 2020.

Moloney, N. R., Faranda, D., and Sato, Y.: An overview of the extremal index, Chaos: An Interdisciplinary Journal of Nonlinear Science, 29, 022 101, 2019.

Mori, M., Watanabe, M., Shiogama, H., Inoue, J., and Kimoto, M.: Robust Arctic sea-ice influence on the frequent Eurasian cold winters in past decades, Nature Geoscience, 7, 869–873, 2014.

Naveau, P., Hannart, A., and Ribes, A.: Statistical methods for extreme event attribution in climate science, Annual Review of Statistics and its Application, 7, 89–110, 2020.

NCDC/NOAA: Billion-Dollar Weather and Climate Disasters, https://www.ncdc.noaa.gov/billions/events/US/2021, accessed: 2022-01-31, 2021.

NCEP/CPC: PSL Data: CPC Unified Gauge-Based Analysis of Daily Precipitation over CONUS RT: NOAA Physical Sciences Laboratory, https://psl.noaa.gov/data/gridded/data.unified.daily.conus.rt.html, accessed: 25-01-2022.

NHC/NOAA: National Hurricane Center - Hurricane KATRINA Advisory Archive, https://www.nhc.noaa.gov/archive/2005/KATRINA.shtml, accessed: 2022-01-31, 2005.

NHC/NOAA: Costliest U.S. tropical cyclones tables updated, https://www.nhc.noaa.gov/news/UpdatedCostliest.pdf, accessed: 2022-01-31, 2018.

NHC/NOAA: National Hurricane Center - Hurricane IDA Advisory Archive, https://www.nhc.noaa.gov/archive/2021/IDA.shtml, accessed: 2022-01-31, 2021.

Ogawa, F., Keenlyside, N., Gao, Y., Koenigk, T., Yang, S., Suo, L., Wang, T., Gastineau, G., Nakamura, T., Cheung, H. N., et al.: Evaluating impacts of recent Arctic sea ice loss on the northern hemisphere winter climate change, Geophysical Research Letters, 45, 3255–3263, 2018.

on Extreme Weather Events, C. and Attribution, C. C.: Attribution of Extreme Weather Events in the Context of Climate Change, https://doi.org/10.17226/21852, 2016.

Pendergrass, A. G., Knutti, R., Lehner, F., Deser, C., and Sanderson, B. M.: Precipitation variability increases in a warmer climate, Scientific reports, 7, 1–9, 2017.

Poli, V. and Stanzani, R.: Rapporto dell'evento meteorologico del 19 e 20 settembre 2021, Arpae Emilia-Romagna - Struttura Idro-Meteo-Clima. Available online at: https://allertameteo.regione.emilia-romagna.it/documents/20181/437770/Evento+19-20+settembre+2021.pdf/ff3ed88f-773d-06e9-eb02-d0a306ae9121?t=1633503536867 (Accessed January 26, 2022), 2022.

Priestley, M. D. K. and Catto, J. L.: Future changes in the extratropical storm tracks and cyclone intensity, wind speed, and structure, Weather and Climate Dynamics, 3, 337–360, https://doi.org/10.5194/wcd-3-337-2022, 2022.

Román-Palacios, C. and Wiens, J. J.: Recent responses to climate change reveal the drivers of species extinction and survival, Proceedings of the National Academy of Sciences, 117, 4211–4217, 2020.

Romero, R. and Emanuel, K.: Climate change and Hurricane-like extratropical cyclones: Projections for North Atlantic polar lows and medicanes based on CMIP5 models, Journal of Climate, 30, 279–299, 2017.

Russo, S. and Sterl, A.: Global changes in indices describing moderate temperature extremes from the daily output of a climate model, Journal of Geophysical Research: Atmospheres, 116, 2011.

Sachweh, M. and Koepke, P.: Radiation fog and urban climate, Geophysical Research Letters, 22, 1073–1076, 1995.

Sainsbury, E. M., Schiemann, R. K., Hodges, K. I., Shaffrey, L. C., Baker, A. J., and Bhatia, K. T.: How important are post-tropical cyclones for European windstorm risk?, Geophysical Research Letters, 47, e2020GL089 853, 2020.

Sarkar, N. and Chaudhuri, B. B.: An efficient differential box-counting approach to compute fractal dimension of image, IEEE Transactions on systems, man, and cybernetics, 24, 115–120, 1994.

Scher, S. and Messori, G.: How global warming changes the difficulty of synoptic weather forecasting, Geophysical Research Letters, 46, 2931–2939, 2019.

Seneviratne, S., Zhang, X., Adnan, M., Badi, W., Dereczynski, C., Luca, A. D., Ghosh, S., Iskandar, I., Kossin, J., Lewis, S., Otto, F., Pinto, I., Satoh, M., Vicente-Serrano, S., Wehner, M., , and Zhou, B.: Weather and Climate Extreme Events in a Changing Climate. In Climate Change 2021: The Physical Science Basis. Contribution of Working Group I to the Sixth Assessment Report of the Intergovernmental Panel on Climate Change, 2021.

Seneviratne, S.I., X. Z. M. A. W. B. C. D. A. D. L. S. G. I. I. J. K. S. L. F. O. I. P. M. S. S. V.-S. M. W. and Zhou, B.: Climate change 2021: the physical science basis, Contribution of working group I to the sixth assessment report of the intergovernmental panel on climate change, p. 2, 2021.

Sharmila, S. and Walsh, K.: Recent poleward shift of tropical cyclone formation linked to Hadley cell expansion, Nature Climate Change, 8, 730–736, 2018.

Shepherd, T. G.: Atmospheric circulation as a source of uncertainty in climate change projections, Nature Geoscience, 7, 703, 2014.

Shepherd, T. G.: A Common Framework for Approaches to Extreme Event Attribution, Current Climate Change Reports, 2, 28–38, https://doi.org/10.1007/s40641-016-0033-y, 2016.

Shepherd, T. G.: Storyline approach to the construction of regional climate change information, Proceedings of the Royal Society A, 475, 20190 013, 2019.

SIAS: Servizio Informativo Agrometeorologico Siciliano, http://www.sias.regione.sicilia.it/frameset_dati.htm, accessed: 2022-01-27, 2021.

SMHI: November 2021 - Nästan rekordkall avslutning, https://www.smhi.se/klimat/klimatet-da-och-nu/manadens-vader-och-vatten-sverige/manadens-vader-i-sverige/november-2021-nastan-rekordkall-avslutning-1.176606, accessed: 2022-01-14, a.

SMHI: November 2021 - La Niña bidrog till översvämningar i sydvästra Kanada, https://www.smhi.se/klimat/klimatet-da-och-nu/manadens-vader-i-varlden/november-2021-la-nina-bidrog-till-oversvamningar-i-sydvastra-kanada-1.176603, accessed: 2022-01-14, b.

Spinoni, J., Barbosa, P., Bucchignani, E., Cassano, J., Cavazos, T., Christensen, J. H., Christensen, O. B., Coppola, E., Evans, J., Geyer, B., Giorgi, F., Hadjinicolaou, P., Jacob, D., Katzfey, J., Koenigk, T., Laprise, R., Lennard, C. J., Kurnaz, M. L., Li, D., Llopart, M., McCormick, N., Naumann, G., Nikulin, G., Ozturk, T., Panitz, H.-J., da Rocha, R. P., Rockel, B., Solman, S. A., Syktus, J., Tangang, F.,

Teichmann, C., Vautard, R., Vogt, J. V., Winger, K., Zittis, G., and Dosio, A.: Future Global Meteorological Drought Hot Spots: A Study Based on CORDEX Data, Journal of Climate, 33, 3635 – 3661, https://doi.org/10.1175/JCLI-D-19-0084.1, 2020.

Stefanon, M., D'Andrea, F., and Drobinski, P.: Heatwave classification over Europe and the Mediterranean region, Environmental Research Letters, 7, 014 023, 2012.

Stendel, M., Francis, J., White, R., Williams, P. D., and Woollings, T.: The jet stream and climate change, in: Climate Change, pp. 327–357, Elsevier, 2021.

Süveges, M.: Likelihood estimation of the extremal index, Extremes, 10, 41–55, 2007.

SVD: Oväder drar österut – flera trafikolyckor, https://www.svd.se/fortsatta-snoproblem-i-soder, accessed: 2022-01-14.

SVT: Tågtrafik i Norrbotten ställs in – för kallt att köra, https://www.svt.se/nyheter/lokalt/norrbotten/tagtrafik-i-norrbotten-stalls-in-for-kallt-att-kora, accessed: 2022-01-14.

Taleb, N.: The black swan: Why don't we learn that we don't learn, NY: Random House, 2005.

Tamarin-Brodsky, T., Hodges, K., Hoskins, B. J., and Shepherd, T. G.: A Dynamical Perspective on Atmospheric Temperature Variability and Its Response to Climate Change, Journal of Climate, 32, 1707–1724, 2019.

Tous, M., Zappa, G., Romero, R., Shaffrey, L., and Vidale, P. L.: Projected changes in medicanes in the HadGEM3 N512 high-resolution global climate model, Climate Dynamics, 47, 1913–1924, 2016.

Trenberth, K. E.: Attribution of climate variations and trends to human influences and natural variability, Wiley Interdisciplinary Reviews: Climate Change, 2, 925–930, 2011.

Trenberth, K. E. and Shea, D. J.: Atlantic hurricanes and natural variability in 2005, Geophysical research letters, 33, 2006.

Trenberth, K. E., Fasullo, J. T., and Shepherd, T. G.: Attribution of climate extreme events, Nature Clim. Change, 5, 725–730, http://dx.doi.org/10.1038/nclimate2657, 2015.

Trisos, C. H., Merow, C., and Pigot, A. L.: The projected timing of abrupt ecological disruption from climate change, Nature, 580, 496–501, 2020.

Ulbrich, U., Leckebusch, G. C., and Pinto, J. G.: Extra-tropical cyclones in the present and future climate: a review, Theoretical and Applied Climatology volume, 96, 117–131, 2009.

Van Oldenborgh, G. J. and Van Ulden, A.: On the relationship between global warming, local warming in the Netherlands and changes in circulation in the 20th century, International Journal of Climatology, 23, 1711–1724, <GotoISI>://000186918700003, 2003.

Van Oldenborgh, G. J., Van Urk, A., and Allen, M.: The absence of a role of climate change in the 2011 Thailand floods, Bull. Amer. Meteor. Soc, 93, 1047–1049, 2012.

Van Oldenborgh, G. J., Mitchell-Larson, E., Vecchi, G. A., De Vries, H., Vautard, R., and Otto, F.: Cold waves are getting milder in the northern midlatitudes, Environmental Research Letters, 14, 114 004, 2019.

van Oldenborgh, G. J., van der Wiel, K., Kew, S., Philip, S., Otto, F., Vautard, R., King, A., Lott, F., Arrighi, J., Singh, R., et al.: Pathways and pitfalls in extreme event attribution, Climatic Change, 166, 1–27, 2021.

Vautard, R. and Yiou, P.: ATTRIBUTION Robustness of warming attribution, Nature Climate Change, 2, 26–27, <GotoISI>://000299495500014, 2012.

Vautard, R., Yiou, P., Otto, F., Stott, P., Christidis, N., Oldenborgh, G. J. v., and Schaller, N.: Attribution of human-induced dynamical and thermodynamical contributions in extreme weather events, Environmental Research Letters, 11, 114 009, http://stacks.iop.org/1748-9326/11/i=11/a=114009, 2016.

Vautard, R., Colette, A., Van Meijgaard, E., Meleux, F., Jan van Oldenborgh, G., Otto, F., Tobin, I., and Yiou, P.: Attribution of Wintertime Anticyclonic Stagnation Contributing to Air Pollution in Western Europe, Bulletin of the American Meteorological Society, 99, S70–S75, 2018.

Vautard, R., van Oldenborg, G., Bonnet, R., Li, S., Robin, Y., Kew, S., Philip, S., Soubeyroux, J., Dubuisson, B., N, V., RIechstein, M., and Otto, F.: Human influence on growing period frosts like the early april 2021 in Central France, https://www.worldweatherattribution.org/wp-content/uploads/GrowingPeriodFrost2021.pdf, accessed: 2022-01-31, 2021.

Walker, E., Mitchell, D., and Seviour, W.: The numerous approaches to tracking extratropical cyclones and the challenges they present, Weather, 75, 336–341, 2020.

Wehrli, K., Hauser, M., and Seneviratne, S. I.: Storylines of the 2018 Northern Hemisphere heatwave at pre-industrial and higher global warming levels, Earth System Dynamics, 11, 855–873, 2020.

WMO: world meteorological organisation, https://public.wmo.int/fr/medias/communiqués-de-presse/état-du-climat-en-2021-des-phénomènes-météorologiques-extrêmes-et-de, accessed: 2022-01-27, 2021.

Ye, K. and Messori, G.: Two leading modes of wintertime atmospheric circulation drive the recent warm Arctic–cold Eurasia temperature pattern, Journal of Climate, 33, 5565–5587, 2020.

Yiou, P., Jézéquel, A., Naveau, P., Otto, F. E. L., Vautard, R., and Vrac, M.: A statistical framework for conditional extreme event attribution, Advances in Statistical Climatology, Meteorology and Oceanography, 3, 17–31, https://doi.org/10.5194/ascmo-3-17-2017, 2017.

Yiou, S., Balembois, F., Schaffers, K., and Georges, P.: Efficient laser operation of an Yb : S-FAP crystal at 985 nm, APPLIED OPTICS, 42, 4883–4886, <GotoISI>://000184940000014, 2003.

Zappa, G., Shaffrey, L. C., Hodges, K. I., Sansom, P. G., , and Stephenson, D. B.: A Multimodel Assessment of Future Projections of North Atlantic and European Extratropical Cyclones in the CMIP5 Climate Models, Journal of Climate, p. 5846–5862, 2013.

Zscheischler, J., Martius, O., Westra, S., Bevacqua, E., Raymond, C., Horton, R. M., van den Hurk, B., AghaKouchak, A., Jézéquel, A., and Mahecha, M. D.: A typology of compound weather and climate events, Nature reviews earth & environment, pp. 1–15, iSBN: 2662-138X Publisher: Nature Publishing Group, 2020.

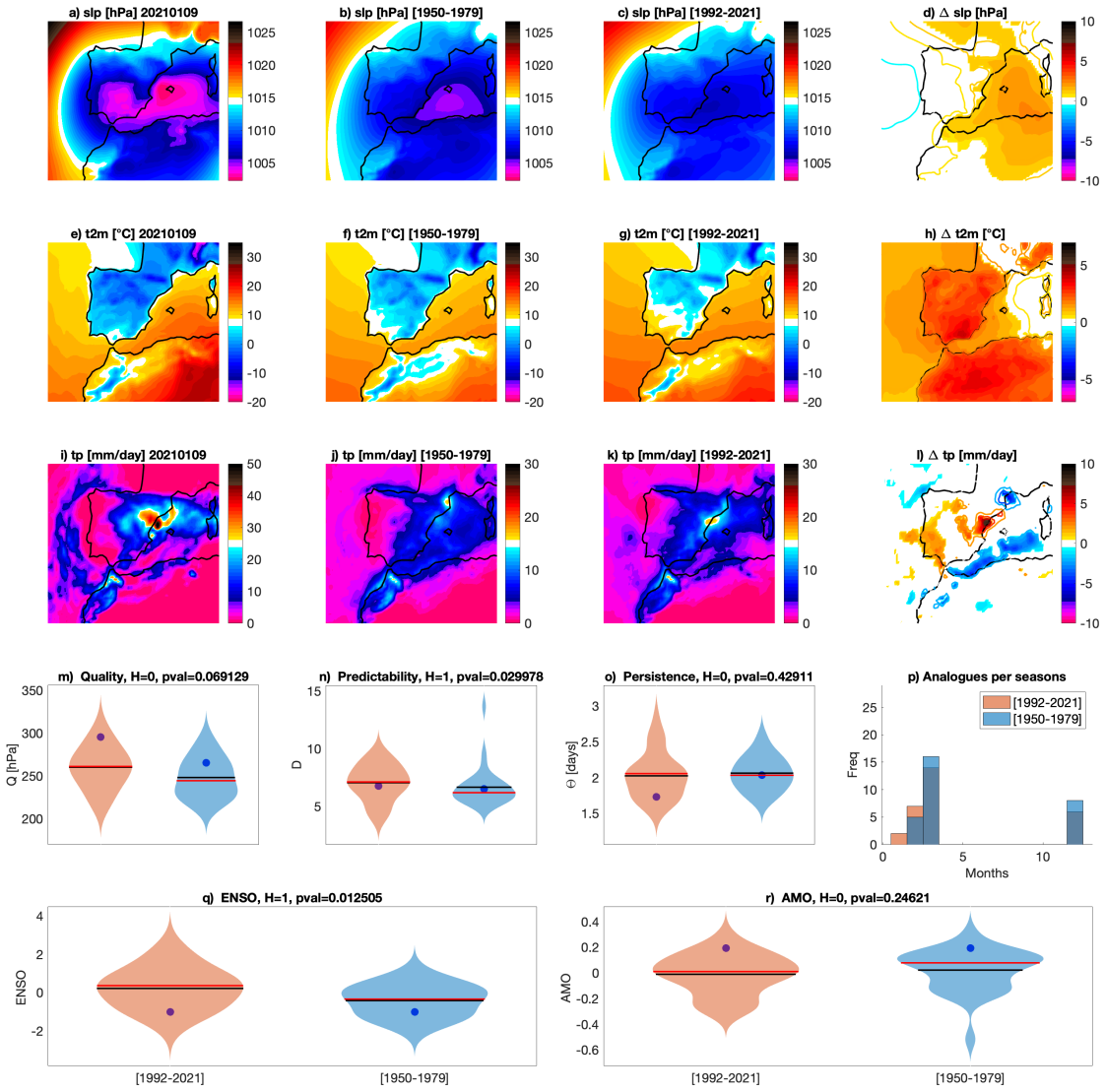

Figure 2. Attribution for Filomena Storm on 09-01-2021. Daily mean sea-level pressure slp (a), 2-meter temperatures $t2m$ (e) and total precipitation tp (i) on the day of the event. Average of the 33 sea-level pressure ~~analogs~~ analogues found for the counterfactual [1950-1979] (b) and factual [1992-2021] (c) periods and corresponding 2-meter temperatures (f,g) and daily precipitation rate (j,k). Δslp (d), $\Delta t2m$ (h) and Δtp (i) between factual and counterfactual periods: colored-filled areas show significant anomalies with respect to the bootstrap procedure. Violin plots for counterfactual (blue) and factual (~~pink~~orange) periods for the ~~Analogs~~ analogues Quality Q (m) the Predictability index D (n), the Persistence index Θ (o) and the distribution of ~~analogs~~ analogues in each month (p). Violin plots for counterfactual (blue) and factual (orange) periods for ENSO (q) and AMO (r). Values for the ~~selected~~ peak day of the extreme event are marked by a blue dot.

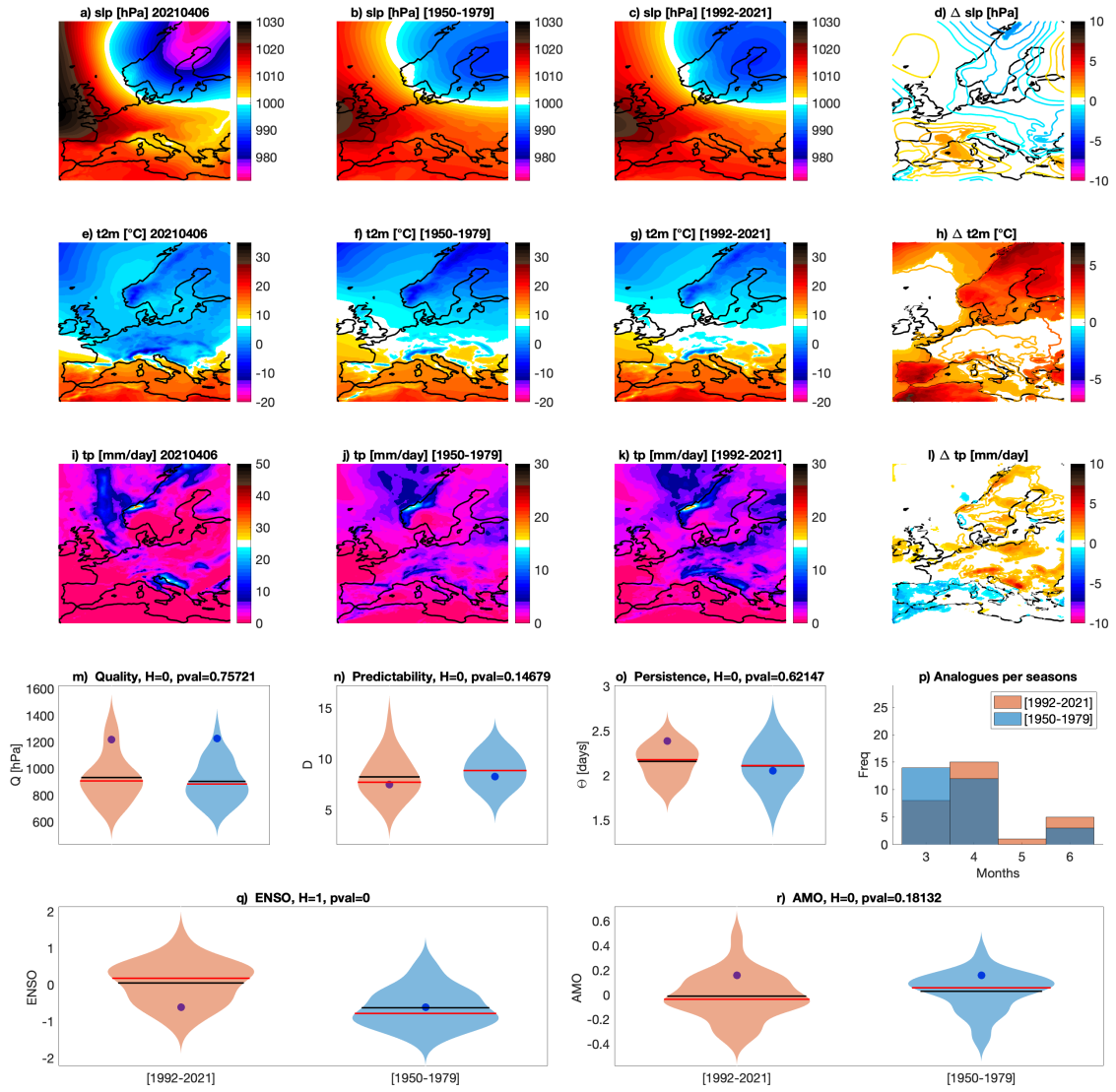

Figure 3. Attribution for the French cold spell on 06-04-2021. Daily mean sea-level pressure slp (a), 2-meter temperatures $t2m$ (e) and total precipitation tp (i) on the day of the event. Average of the 33 sea-level pressure ~~analogs~~ analogues found for the counterfactual [1950-1979] (b) and factual [1992-2021] (c) periods and corresponding 2-meter temperatures (f,g) and daily precipitation rate (j,k). Δslp (d), $\Delta t2m$ (h) and Δtp (i) between factual and counterfactual periods: colored-filled areas show significant anomalies with respect to the bootstrap procedure. Violin plots for counterfactual (blue) and factual (~~pink~~orange) periods for the ~~Analogs~~ analogues Quality Q (m) the Predictability index D (n), the Persistence index Θ (o) and the distribution of ~~analogs~~ analogues in each month (p). Violin plots for counterfactual (blue) and factual (orange) periods for ENSO (q) and AMO (r) indices. Values for the ~~selected~~ peak day of the extreme event are marked by a blue dot. Horizontal bars in panels (m–r) correspond to the mean (black) and median (red) of the distributions.

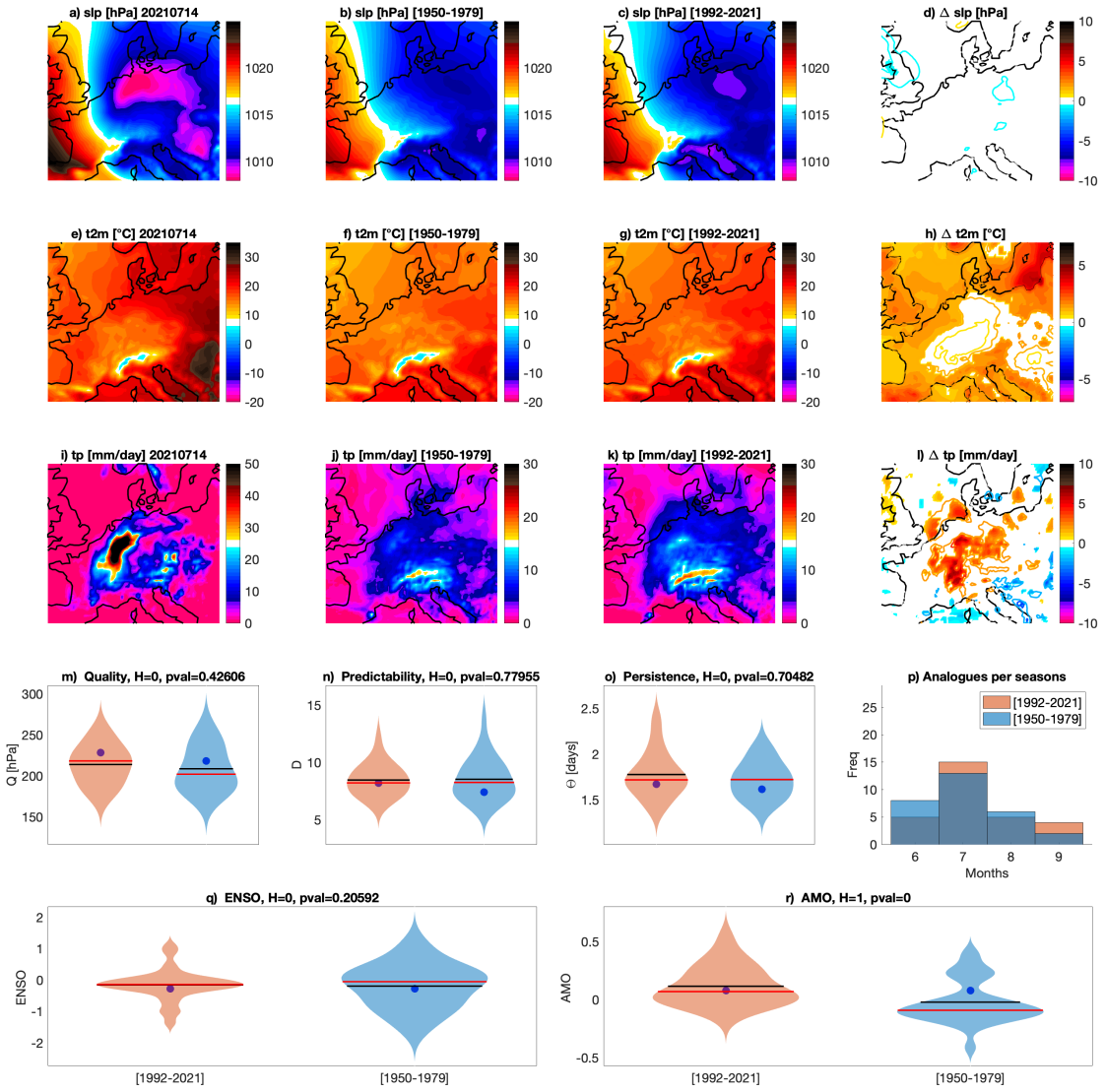

Figure 4. Attribution for the Westphalia Floods on 14-07-2021. Daily mean sea-level pressure slp (a), 2-meter temperatures $t2m$ (e) and total precipitation tp (i) on the day of the event. Average of the 33 sea-level pressure ~~analogs~~ analogues found for the counterfactual [1950-1979] (b) and factual [1992-2021] (c) periods and corresponding 2-meter temperatures (f,g) and daily precipitation rate (j,k). Δslp (d), $\Delta t2m$ (h) and Δtp (i) between factual and counterfactual periods: colored-filled areas show significant anomalies with respect to the bootstrap procedure. Violin plots for counterfactual (blue) and factual (~~pink~~orange) periods for the ~~Analogs~~ analogues Quality Q (m) the Predictability index D (n), the Persistence index Θ (o) and the distribution of ~~analogs~~ analogues in each month (p). Violin plots for counterfactual (blue) and factual (orange) periods for ENSO (q) and AMO (r). Values for the ~~selected~~ peak day of the extreme event are marked by a blue dot. Horizontal bars in panels (m–r) correspond to the mean (black) and median (red) of the distributions.

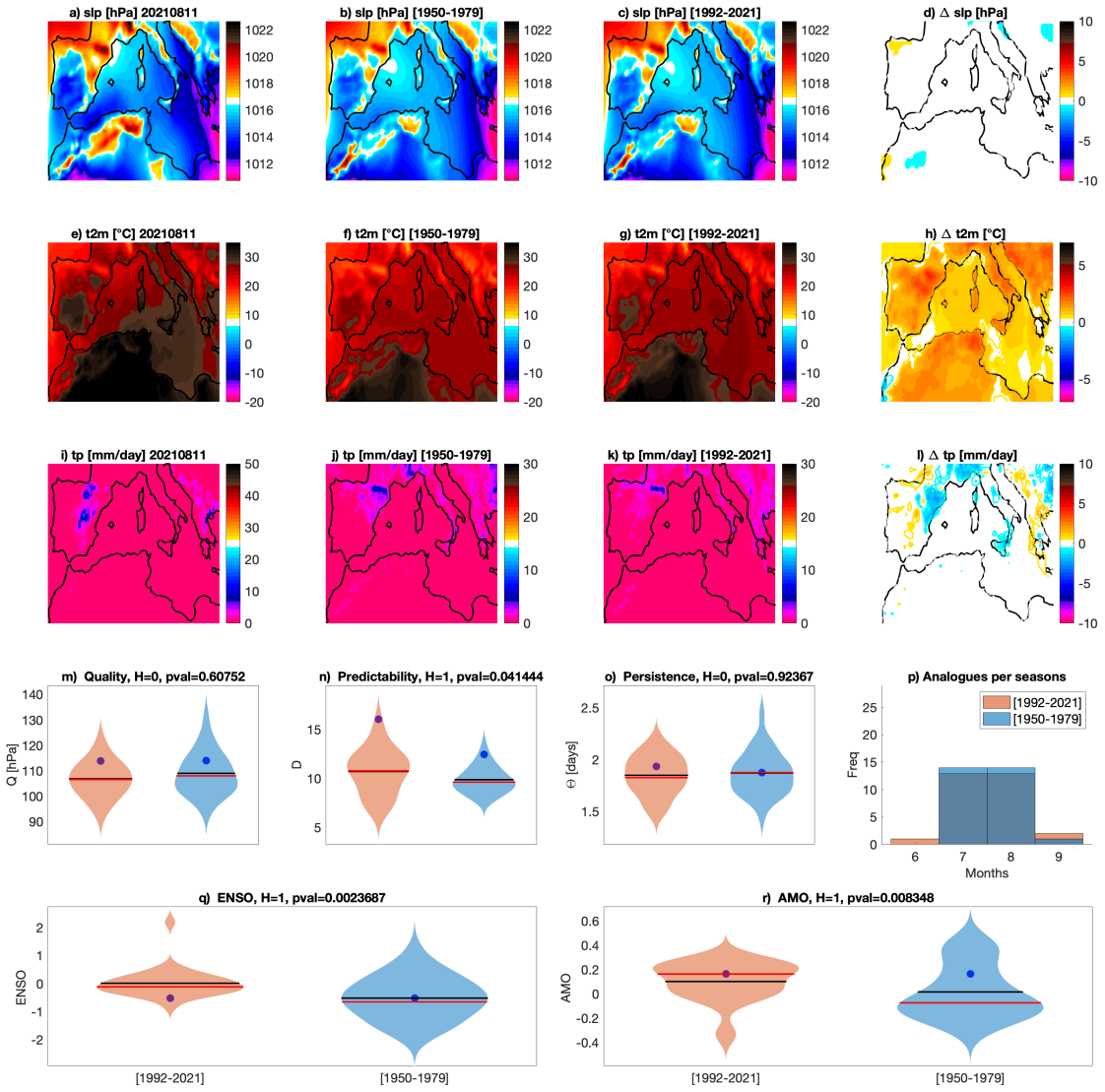

Figure 5. Attribution for the Mediterranean Heat Peak on 11-08-2021. Daily mean sea-level pressure slp (a), 2-meter temperatures $t2m$ (e) and total precipitation tp (i) on the day of the event. Average of the 33 sea-level pressure ~~analogs~~ analogues found for the counterfactual [1950-1979] (b) and factual [1992-2021] (c) periods and corresponding 2-meter temperatures (f,g) and daily precipitation rate (j,k). Δslp (d), $\Delta t2m$ (h) and Δtp (i) between factual and counterfactual periods: colored-filled areas show significant anomalies with respect to the bootstrap procedure. Violin plots for counterfactual (blue) and factual (~~pink~~orange) periods for the ~~Analogs~~ analogues Quality Q (m) the Predictability index D (n), the Persistence index Θ (o) and the distribution of ~~analogs~~ analogues in each month (p). Violin plots for counterfactual (blue) and factual (orange) periods for ENSO (q) and AMO (r). Values for the ~~selected~~ peak day of the extreme event are marked by a blue dot. Horizontal bars in panels (m–r) correspond to the mean (black) and median (red) of the distributions.

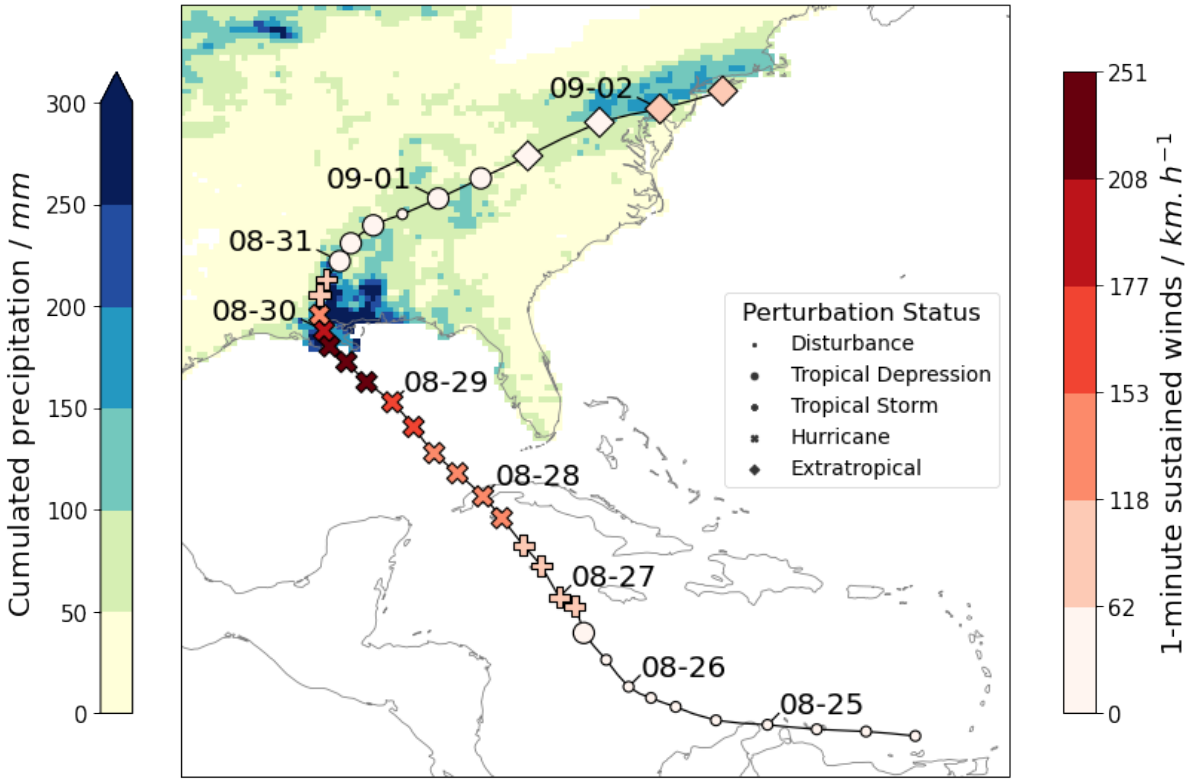

Figure 6. Track and associated precipitation for ~~the Ida~~ hurricane Ida. 6-hourly track position from the IBTrACS (Knapp et al., 2010; Knapp, Kenneth R et al., 2018) ~~)~~ database are provided with their wind speed ~~an~~ and status from the NHC report. Time stamps are UTC, format mm-dd. Cumulated daily precipitation between 28-08-2021 and 03-09-2021 from the NCEP/CPC US Unified Precipitation are displayed. White ~~color~~ indicates no data~~in the figure~~.

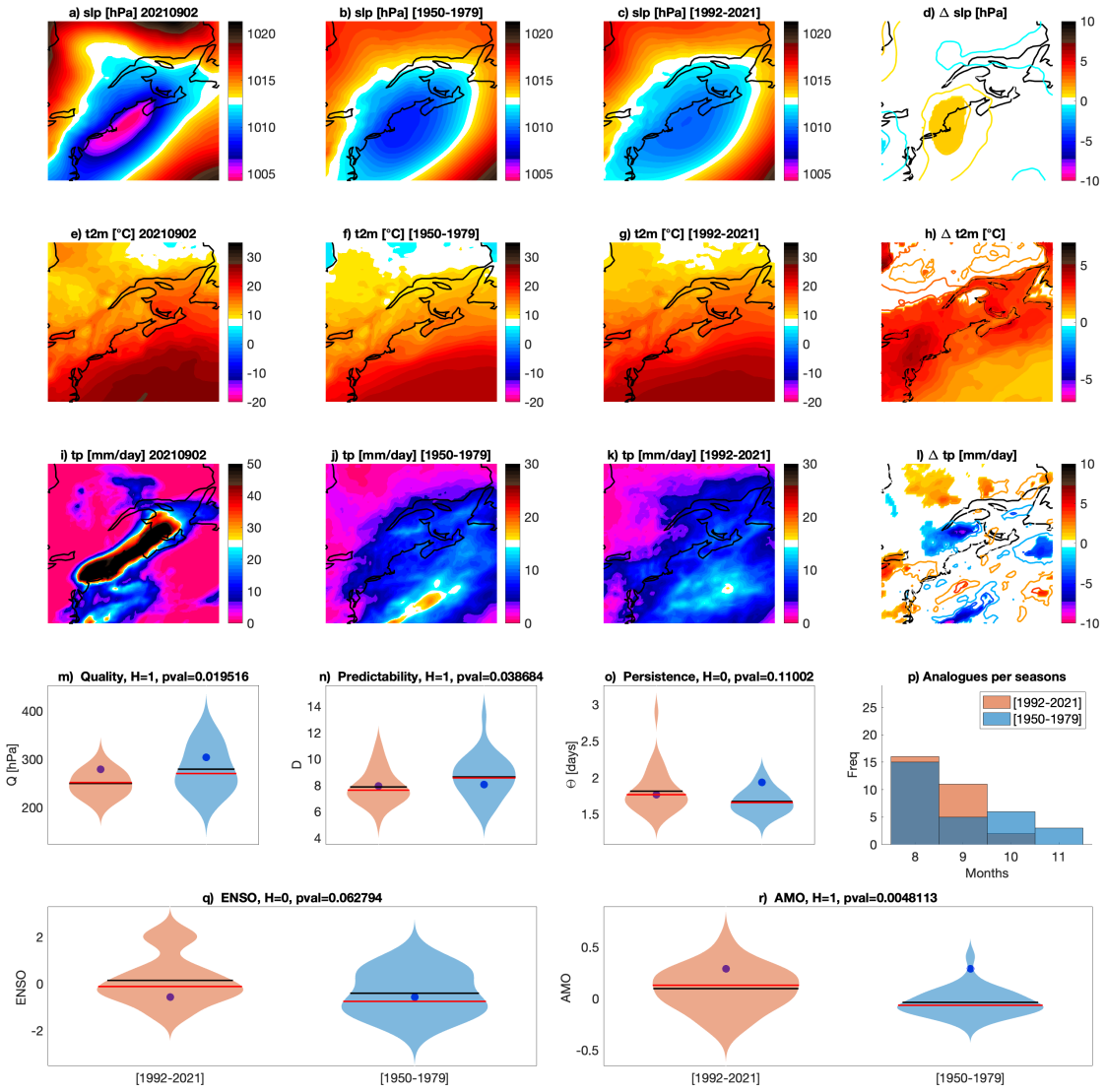

Figure 7. Attribution for the Hurricane Ida passage over New-York City area on 02-09-2021. Daily mean sea-level pressure slp (a), 2-meter temperatures $t2m$ (e) and total precipitation tp (i) on the day of the event. Average of the 33 sea-level pressure ~~analogs~~ analogues found for the counterfactual [1950-1979] (b) and factual [1992-2021] (c) periods and corresponding 2-meter temperatures (f,g) and daily precipitation rate (j,k). Δslp (d), $\Delta t2m$ (h) and Δtp (i) between factual and counterfactual periods: colored-filled areas show significant anomalies with respect to the bootstrap procedure. Violin plots for counterfactual (blue) and factual (~~pink~~orange) periods for the ~~Analogs~~ analogues Quality Q (m) the Predictability index D (n), the Persistence index Θ (o) and the distribution of ~~analogs~~ analogues in each month (p). Violin plots for counterfactual (blue) and factual (orange) periods for ENSO (q) and AMO (r). Values for the ~~selected~~ peak day of the extreme event are marked by a blue dot. Horizontal bars in panels (m–r) correspond to the mean (black) and median (red) of the distributions.

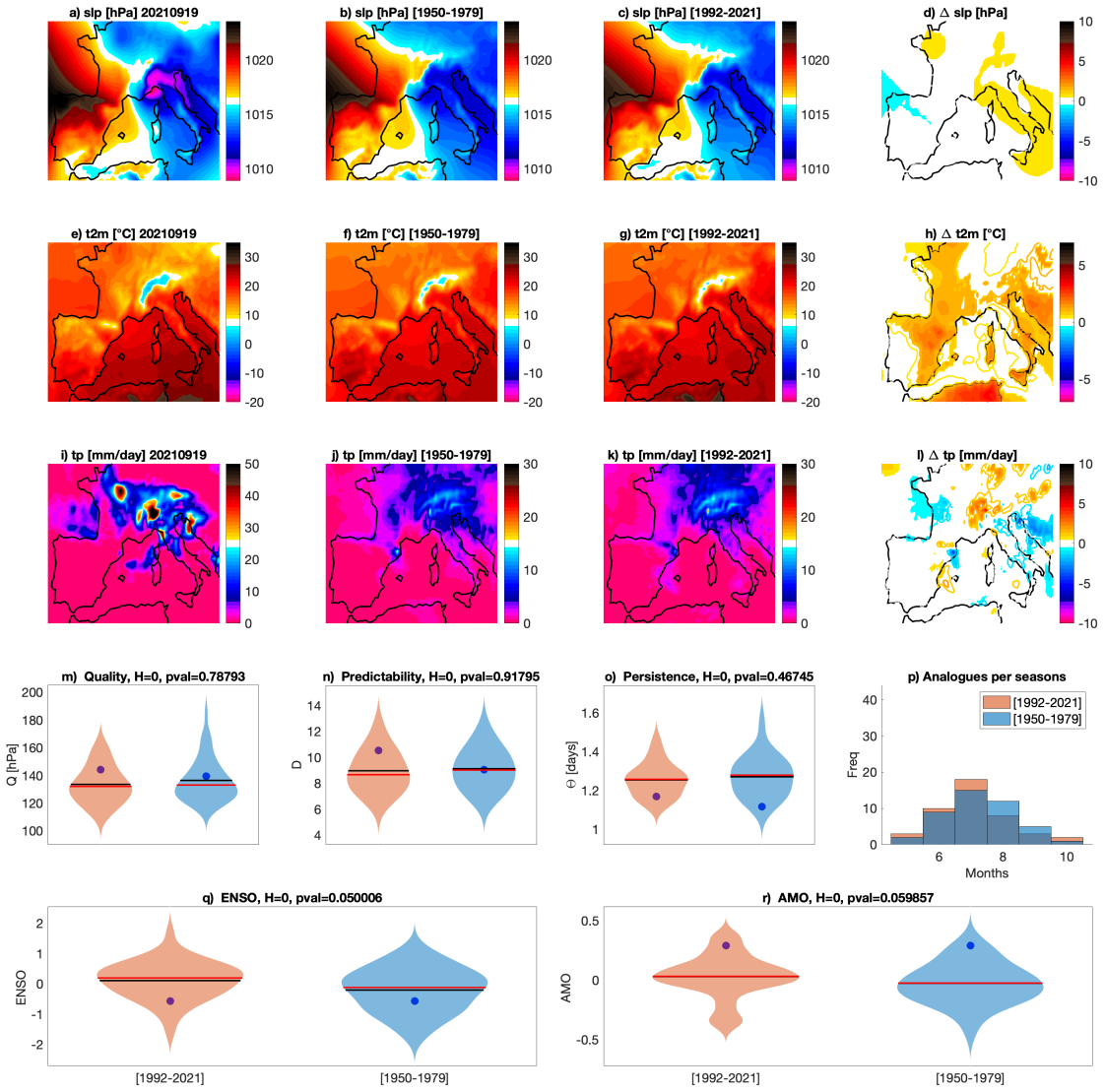

Figure 8. Attribution for the Po Valley Tornadoes ~~Outbreak~~ Outbreak on 19-09-2021. Daily mean sea-level pressure slp (a), 2-meter temperatures $t2m$ (e) and total precipitation tp (i) on the day of the event. Average of the 33 sea-level pressure ~~analogs~~ analogues found for the counterfactual [1950-1979] (b) and factual [1992-2021] (c) periods and corresponding 2-meter temperatures (f,g) and daily precipitation rate (j,k). Δslp (d), $\Delta t2m$ (h) and Δtp (i) between factual and counterfactual periods: colored-filled areas show significant anomalies with respect to the bootstrap procedure. Violin plots for counterfactual (blue) and factual (~~pink~~orange) periods for the ~~Analogs~~ analogues Quality Q (m) the Predictability index D (n), the Persistence index Θ (o) and the distribution of ~~analogs~~ analogues in each month (p). Violin plots for counterfactual (blue) and factual (orange) periods for ENSO (q) and AMO (r). Values for the ~~selected~~ peak day of the extreme event are marked by a blue dot. Horizontal bars in panels (m–r) correspond to the mean (black) and median (red) of the distributions.

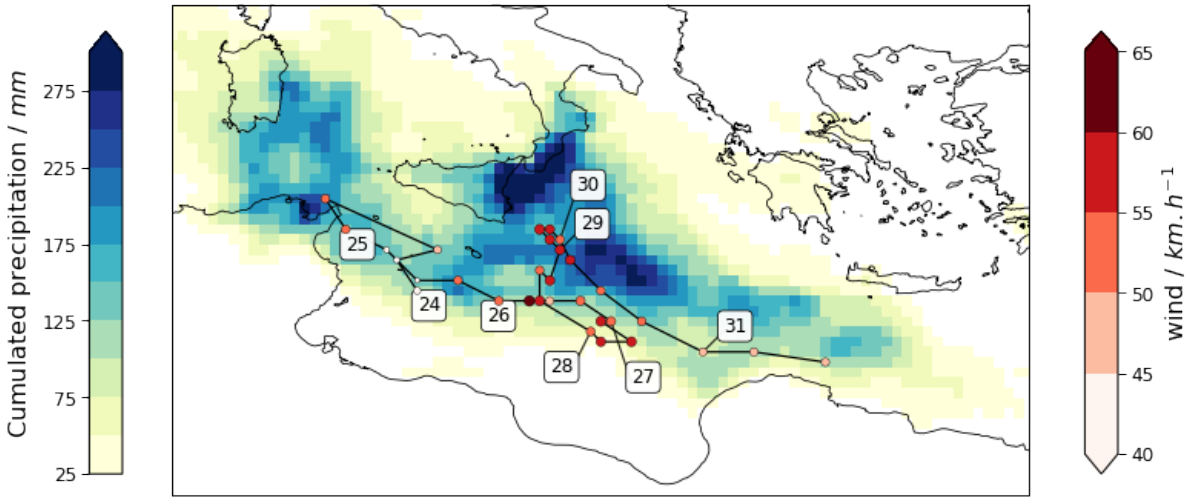

Figure 9. Track and associated precipitation for Apollo. Data from ERA5: Track position is retrieved as the local minimum of *slp*, wind is the maximum wind speed in a 1.5° GCD radius of the slp center, ~~cumulated~~ precipitation is cumulated between 00 UTC on 24-10-2021 and 16 UTC 31-10-2021. Time stamps ~~are UTC, format mm-dd~~indicate the first point for each day whose number is indicated.

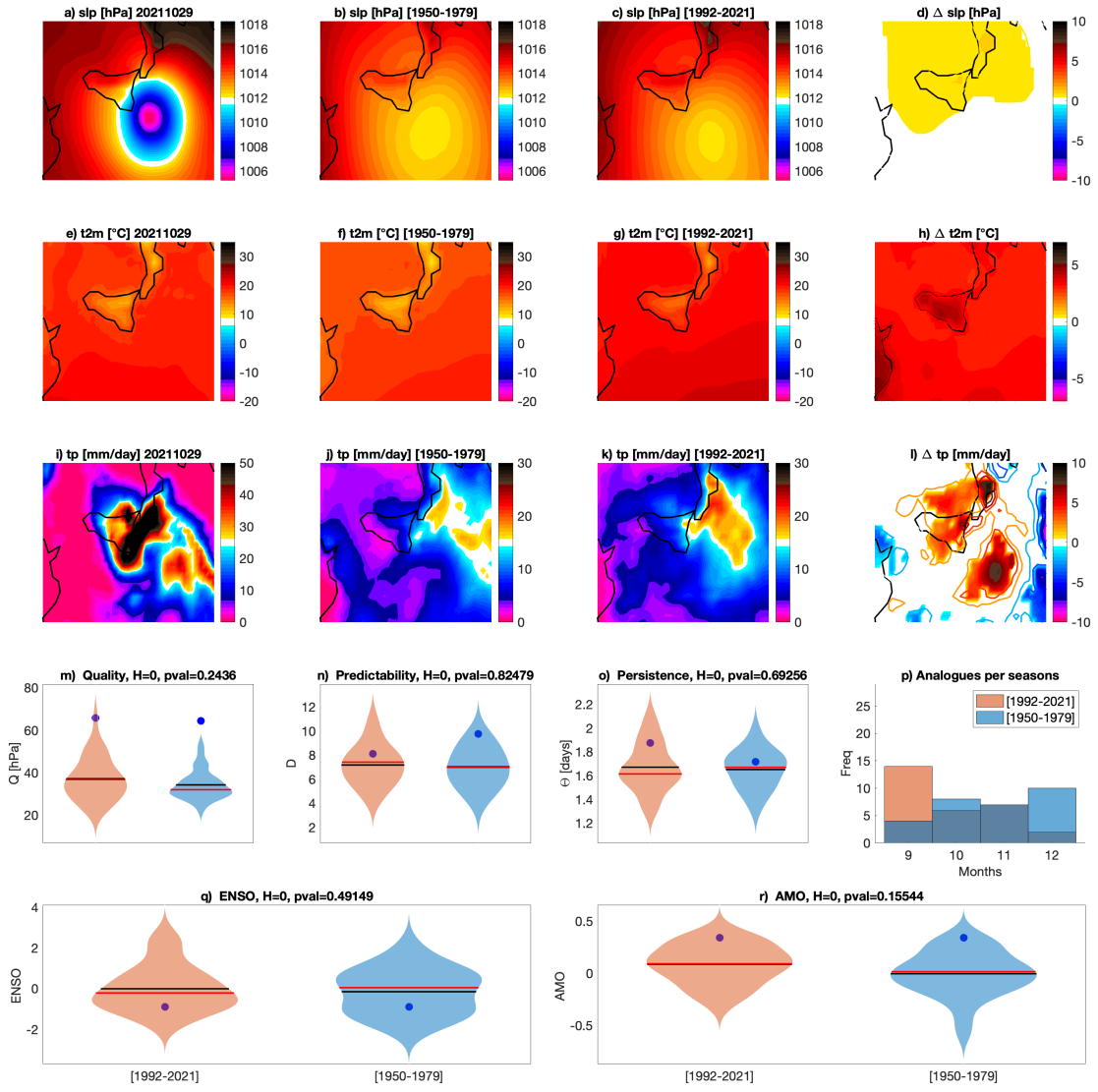

Figure 10. Attribution for the Medicane Apollo on 29-10-2021. Daily mean sea-level pressure slp (a), 2-meter temperatures $t2m$ (e) and total precipitation tp (i) on the day of the event. Average of the 33 sea-level pressure ~~analogs~~ analogues found for the counterfactual [1950-1979] (b) and factual [1992-2021] (c) periods and corresponding 2-meter temperatures (f,g) and daily precipitation rate (j,k). Δslp (d), $\Delta t2m$ (h) and Δtp (i) between factual and counterfactual periods: colored-filled areas show significant anomalies with respect to the bootstrap procedure. Violin plots for counterfactual (blue) and factual (~~pink~~orange) periods for the ~~Analogs~~ analogues Quality Q (m) the Predictability index D (n), the Persistence index Θ (o) and the distribution of ~~analogs~~ analogues in each month (p). Violin plots for counterfactual (blue) and factual (orange) periods for ENSO (q) and AMO (r). Values for the ~~selected~~ peak day of the extreme event are marked by a blue dot. Horizontal bars in panels (m–r) correspond to the mean (black) and median (red) of the distributions.

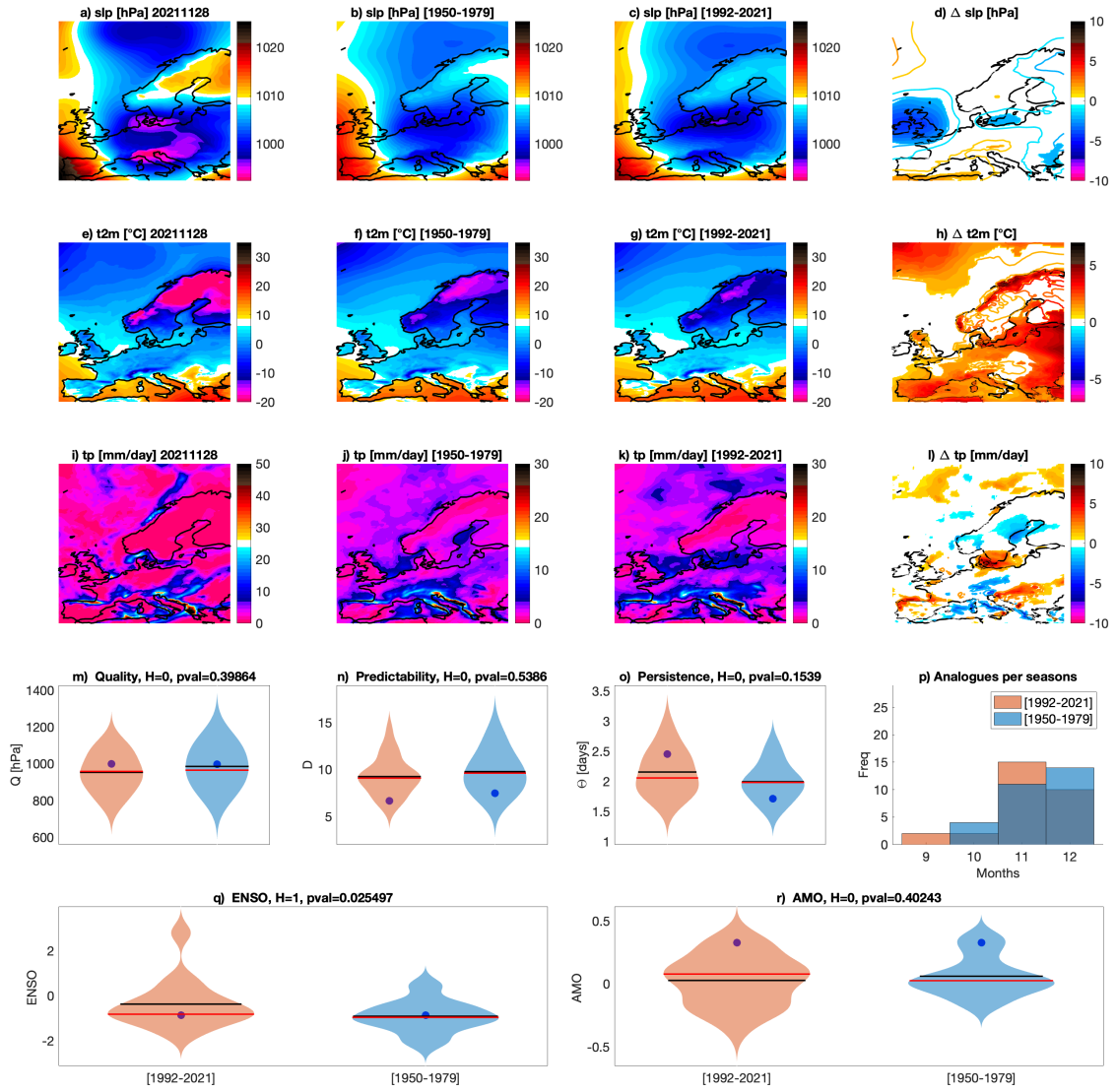

Figure 11. Attribution for the Scandinavian Cold Spell on 28-11-2021. Daily mean sea-level pressure slp (a), 2-meter temperatures $t2m$ (e) and total precipitation tp (i) on the day of the event. Average of the 33 sea-level pressure ~~analogs~~ analogues found for the counterfactual [1950-1979] (b) and factual [1992-2021] (c) periods and corresponding 2-meter temperatures (f,g) and daily precipitation rate (j,k). Δslp (d), $\Delta t2m$ (h) and Δtp (i) between factual and counterfactual periods: colored-filled areas show significant anomalies with respect to the bootstrap procedure. Violin plots for counterfactual (blue) and factual (~~pink~~orange) periods for the ~~Analogs~~ analogues Quality Q (m) the Predictability index D (n), the Persistence index Θ (o) and the distribution of ~~analogs~~ analogues in each month (p). Violin plots for counterfactual (blue) and factual (orange) periods for ENSO (q) and AMO (r). Values for the ~~selected~~ peak day of the extreme event are marked by a blue dot. Horizontal bars in panels (m–r) correspond to the mean (black) and median (red) of the distributions.